PARAXIAL COUPLING OF ELECTROMAGNETIC WAVES IN RANDOM MEDIA

JOSSELIN GARNIER* AND KNUT SØLNA†

Abstract. We consider the propagation of temporally pulsed electromagnetic waves in a three-dimensional random medium. The main objective is to derive effective white-noise paraxial equations from Maxwell's equations. We address the scaling regime in which 1) the carrier wavelength is small compared to the incident beam radius, which is itself small compared to the propagation distance; 2) the correlation length of the fluctuations of the random medium is of the same order as the beam radius, and the typical amplitude of the fluctuations is small. In this regime we prove that the wave field is characterized by a white-noise paraxial wave equation that has the form of a Schrödinger-type equation driven by a Brownian field. We identify the covariance function of the Brownian field in terms of the two-point statistics of the fluctuations of the dielectric permittivity and the magnetic permeability of the medium. We also study the case in which a strong interface is embedded in the random medium and study the reflected wave, which again is characterized by a Schrödinger-type equation. We discuss applications to enhanced backscattering, time reversal, and imaging.

Key words. Electromagnetic waves, parabolic approximation, enhanced backscattering, random media

1. Introduction. In the last decades the parabolic or paraxial wave equation has emerged as the primary tool to describe small scale scattering situations as they appear in radiowave propagation, radar, remote sensing, seismic imaging, wireless communication, propagation in urban environments, and in underwater acoustics [7, 26, 32], as well as in propagation problems in the earth's crust [9]. The paraxial equation models wave propagation if the dominant scattering occurs in the direction(s) transverse to a principal propagation direction in the situation with a privileged propagation axis. It was first introduced by Leontovitch and Fock [18] and it is now used for many applications. In the case of scalar waves in heterogeneous media, the time-harmonic field is the solution of a Schrödinger equation in which the evolution variable is the spatial variable along the privileged propagation axis, and the heterogeneous medium plays the role of a random potential. This Schrödinger or paraxial wave equation is obtained by neglecting backscattering. It is simple compared to the full three-dimensional wave equation (or the Helmholtz equation for the time-harmonic field) since it is a one-way equation, and it enables analysis of many wave phenomena, such as laser beam propagation [31].

However, it is not possible to obtain closed-form equations for the moments of the wave field when the random fluctuations of the medium are arbitrary. The latter can be achieved by using the white-noise approximation. The white-noise paraxial wave equation is of interest for at least two reasons [21, 33]. First, it appears as a natural model when the correlation length of the fluctuations of the medium is smaller than the propagation distance. Second it allows for the use of Itô's stochastic calculus, which in turn enables the closure of the hierarchy of moment equations and the statistical analysis of important wave propagation problems, such as scintillation [20]. When the paraxial approximation and the white-noise approximation can be justified simultaneously for scalar waves, then the limit equation takes the form of the random Schrödinger equation driven by a Brownian field studied in particular in

*Laboratoire de Probabilités et Modèles Aléatoires & Laboratoire Jacques-Louis Lions, Université Paris 7, 2 Place Jussieu, 75251 Paris Cedex 05, France, garnier@math.jussieu.fr.

†Department of Mathematics, University of California at Irvine, Irvine, CA 92697-3875, USA ksolna@math.uci.edu

[10]. The proof of the convergence of the solution of the wave equation in random media to the solution of the white-noise paraxial equation was obtained for stratified weakly fluctuating media in [4] and recently for three-dimensional random media in the context of acoustic waves in [24]. Despite its importance and many applications a rigorous derivation of the paraxial approximation for electromagnetic waves in heterogeneous media in the scaling limit where the potential takes the form of a Brownian flow has thus far not been presented. Our paper extends the scalar, acoustic theory that we developed in Ref. [24] to the vector, electromagnetic case. We will show that electromagnetic wave propagation in a certain regime can be described by a system of Schrödinger equations driven by a single Brownian field. The proof involves invariant imbedding and diffusion approximation theorems, which were used for instance in [25] to analyze the reflection of electromagnetic waves from a randomly stratified half-space in a different scaling regime. We will identify the covariance function of the Brownian field in terms of the two-point statistics of the fluctuations of the dielectric permittivity and the magnetic permeability. Moreover, our results show how the electromagnetic wave modes decouple dynamically justifying the scalar wave approximation often used in applications. However, our analysis shows for the first time how the modes couple statistically. This statistical coupling is very important in certain applications such as time reversal of electromagnetic waves that we address in our paper. We will also consider the case in which a strong interface is present in the random medium, which is a configuration of interest for optical tomography [34]. We will show that the reflected field can be described by a Schrödinger-type equation which accounts for all incoherent and coherent effects, such as enhanced backscattering.

The paper is organized as follows. In Section 2 we describe the Maxwell's equations in a random medium. We introduce the decomposition into 'right' and 'left' propagating modes in Section 3. In Section 4 we present the main results regarding random paraxial wave equations. The proofs of the results are given in Section 5. A convenient tool for analysis of wave field moments is the Wigner transform of the fields and we introduce this in Section 6. We use this tool for the analysis of enhanced backscattering and time reversal in Section 7.

2. Maxwell's equations for electromagnetic waves in a random medium. We consider electromagnetic waves propagating in a three-dimensional medium with heterogeneous random fluctuations and without dispersion. Maxwell's equations for the electric field $\boldsymbol{E}(t,\boldsymbol{x},z)$ and the magnetic field strength $\boldsymbol{H}(t,\boldsymbol{x},z)$ are

$$\nabla\times\boldsymbol{E}=-\mu(\boldsymbol{x},z)\partial_t\boldsymbol{H}, \tag{2.1}$$

$$\nabla\cdot(\varepsilon(\boldsymbol{x},z)\boldsymbol{E})=\rho(t,\boldsymbol{x},z), \tag{2.2}$$

$$\nabla\times\boldsymbol{H}=\boldsymbol{J}^{(s)}(t,\boldsymbol{x},z)+\varepsilon(\boldsymbol{x},z)\partial_t\boldsymbol{E}, \tag{2.3}$$

$$\nabla\cdot(\mu(\boldsymbol{x},z)\boldsymbol{H})=0. \tag{2.4}$$

Here we denote the spatial variable by $(\boldsymbol{x},z)$, with $\boldsymbol{x}=(x,y)\in\mathbb{R}^2$. The term $\boldsymbol{J}^{(s)}$ is a current source term, ε is the dielectric permittivity of the medium, and μ is the magnetic permeability of the medium. Note that the equation of continuity of charge $\partial_t\rho+\nabla\cdot\boldsymbol{J}^{(s)}=0$ is automatically satisfied.

We consider in this paper the situation in which a random section occupying the region $z\in(0,L)$ is sandwiched in between two homogeneous half-spaces. We denote the medium parameters in the half-space $z<0$ by ε_1 and μ_1 and in the half-space $z>L$ by ε_0 and μ_0. The medium is assumed to be matched at the right boundary $z=L$, while we consider a possible mismatch at the left boundary $z=0$ (in the sense

that $(\varepsilon_1, \mu_1) \neq (\varepsilon_0, \mu_0)$). The medium parameters are:

$$\varepsilon(\boldsymbol{x}, z) = \begin{cases} \varepsilon_1 & \text{if } z \leq 0, \\ \varepsilon_0\big[1 + m_\varepsilon(\boldsymbol{x}, z)\big] & \text{if } z \in (0, L), \\ \varepsilon_0 & \text{if } z \geq L, \end{cases} \tag{2.5}$$

$$\mu(\boldsymbol{x}, z) = \begin{cases} \mu_1 & \text{if } z \leq 0, \\ \mu_0\big[1 + m_\mu(\boldsymbol{x}, z)\big] & \text{if } z \in (0, L), \\ \mu_0 & \text{if } z \geq L. \end{cases} \tag{2.6}$$

The random processes $m_\varepsilon(\boldsymbol{x}, z)$ and $m_\mu(\boldsymbol{x}, z)$ model the medium fluctuations. We assume that they are bounded, stationary, and zero-mean and that they satisfy strong mixing conditions in z.

We now put the problem in dimensionless form. Let $\bar{L}$ denote a typical propagation distance, $\bar{\varepsilon}$ and $\bar{\mu}$ denote typical dielectric permittivity and magnetic permeability, and $\bar{E}$ represent a reference electric field strength. This corresponds to a typical propagation speed $\bar{c} = \bar{\mu}^{-1/2}\bar{\varepsilon}^{-1/2}$ and a typical impedance $\bar{\zeta} = \bar{\mu}^{1/2}\bar{\varepsilon}^{-1/2}$. We define the dimensionless independent variables

$$\boldsymbol{x}' = \bar{L}^{-1}\boldsymbol{x}, \quad z' = \bar{L}^{-1}z, \quad t' = \bar{c}\bar{L}^{-1}t,$$

and the following dimensionless variables:

$$\begin{aligned} &\boldsymbol{E}' = \bar{E}^{-1}\boldsymbol{E}, \quad \varepsilon' = \bar{\varepsilon}^{-1}\varepsilon, \quad \boldsymbol{J}^{(s)\prime} = (\bar{L}\bar{\zeta}\bar{E}^{-1})\boldsymbol{J}^{(s)}, \\ &\boldsymbol{H}' = (\bar{\zeta}\bar{E}^{-1})\boldsymbol{H}, \quad \mu' = \bar{\mu}^{-1}\mu, \quad \rho' = (\bar{L}\bar{\varepsilon}^{-1}\bar{E}^{-1})\rho. \end{aligned}$$

After *dropping* the primes, Maxwell's equations in dimensionless form have the form (2.1-2.4) with

$$\varepsilon(\boldsymbol{x}, z) = \begin{cases} \varepsilon_1 & \text{if } z \leq 0, \\ \varepsilon_0\big[1 + \alpha^3 n_\varepsilon(\frac{\boldsymbol{x}}{\alpha^2}, \frac{z}{\alpha^2})\big] & \text{if } z \in (0, L), \\ \varepsilon_0 & \text{if } z \geq L, \end{cases} \tag{2.7}$$

$$\mu(\boldsymbol{x}, z) = \begin{cases} \mu_1 & \text{if } z \leq 0, \\ \mu_0\big[1 + \alpha^3 n_\mu(\frac{\boldsymbol{x}}{\alpha^2}, \frac{z}{\alpha^2})\big] & \text{if } z \in (0, L), \\ \mu_0 & \text{if } z \geq L. \end{cases} \tag{2.8}$$

The parameter α^2 is the ratio of the correlation length of the random medium fluctuations over the typical propagation distance. We will assume that it is small. Here we have also *assumed* that the amplitude of the random fluctuations is small, of order α^3, because this is the interesting regime in which the effective terms due to the random medium fluctuations are of order one when α goes to zero. The dimensionless random processes $n_\varepsilon(\boldsymbol{x}, z)$ and $n_\mu(\boldsymbol{x}, z)$ have standard deviation and (dimensionless) correlation length of order one.

We assume that the current source $\boldsymbol{J}^{(s)}$ is located at the surface in the plane $z = L$. We consider a scaling regime in which the spatial support of the source (in the transverse direction), which will determine the initial beam width, is of order α^2. This means that the transverse scale of the source and the one of the spatial fluctuations of the medium are of the same order. Remember that the Rayleigh length for a beam with initial beam width r_0 and carrier wavenumber k_0 is of the order of $k_0 r_0^2$ in absence of random fluctuations (the Rayleigh length is the distance from beam waist where the beam area is doubled by diffraction). Therefore, if we assume that the carrier

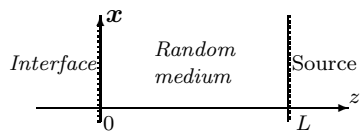

FIG. 2.1. *Schematic of the reflection-transmission problem: a source at $z = L$ emits a wave in the random section $z \in (0, L)$, in the presence of a strong interface at $z = 0$.*

wavelength of the source is of order α^4, then the Rayleigh length is of order one. In this regime the source has the form

$$\boldsymbol{J}^{(s)}(t, \boldsymbol{x}, z) = \boldsymbol{J}\Big(\frac{t}{\alpha^4}, \frac{\boldsymbol{x}}{\alpha^2}\Big)\delta(z - L), \tag{2.9}$$

and it generates waves that propagate mainly along the z-axis, as we will see below. We shall refer to waves propagating in a direction with a negative (resp. positive) z-component as left-going (resp. right-going) waves.

Before starting the analysis of the problem, we discuss the relevance of the scaling hypotheses for a particular case. In an optical context (light beam propagation through the turbulent atmosphere), we may consider the situation in which the carrier wavelength is of the order of 1 μm and the typical propagation distance is of the order of 100 m. The correlation radius of the fluctuations of the medium and the typical beam radius are of the order of 1 cm. Here $\alpha^2 = 10^{-4}$. In order to be in the suitable regime, the amplitude of the fluctuations of the medium should be small, of the order of 10^{-6}, which is indeed the case in the turbulent atmosphere [31].

3. The boundary value problem for the wave modes. We rescale the transverse spatial variables and the time variable so as to observe the wave at the scale of the source and we take a Fourier transform in time:

$$\breve{\boldsymbol{E}}^{\alpha}(\omega, \boldsymbol{x}, z) = \int \boldsymbol{E}(\alpha^4 t, \alpha^2 \boldsymbol{x}, z) e^{i\omega t} \mathrm{d}t, \quad \breve{\boldsymbol{H}}^{\alpha}(\omega, \boldsymbol{x}, z) = \int \boldsymbol{H}(\alpha^4 t, \alpha^2 \boldsymbol{x}, z) e^{i\omega t} \mathrm{d}t.$$

We denote $\breve{\boldsymbol{E}} = (\breve{E}_j)_{j=1,2,3}$ and $\breve{\boldsymbol{H}} = (\breve{H}_j)_{j=1,2,3}$. The four-dimensional vector $(\breve{E}_1^{\alpha}, \breve{H}_2^{\alpha}, \breve{E}_2^{\alpha}, \breve{H}_1^{\alpha})$ satisfies:

$$\partial_z \breve{E}_1^{\alpha} = \frac{i\omega\mu}{\alpha^4}\breve{H}_2^{\alpha} + \frac{i}{\omega}\partial_x\big[\frac{1}{\varepsilon}(\partial_x \breve{H}_2^{\alpha} - \partial_y \breve{H}_1^{\alpha})\big] - \frac{i\alpha^2}{\omega}\partial_x\big[\frac{1}{\varepsilon}\breve{J}_3\big]\delta(z - L), \tag{3.1}$$

$$\partial_z \breve{H}_2^{\alpha} = \frac{i\omega\varepsilon}{\alpha^4}\breve{E}_1^{\alpha} - \frac{i}{\omega}\partial_y\big[\frac{1}{\mu}(\partial_x \breve{E}_2^{\alpha} - \partial_y \breve{E}_1^{\alpha})\big] - \breve{J}_1\delta(z - L), \tag{3.2}$$

$$\partial_z \breve{E}_2^{\alpha} = -\frac{i\omega\mu}{\alpha^4}\breve{H}_1^{\alpha} + \frac{i}{\omega}\partial_y\big[\frac{1}{\varepsilon}(\partial_x \breve{H}_2^{\alpha} - \partial_y \breve{H}_1^{\alpha})\big] - \frac{i\alpha^2}{\omega}\partial_y\big[\frac{1}{\varepsilon}\breve{J}_3\big]\delta(z - L), \tag{3.3}$$

$$\partial_z \breve{H}_1^{\alpha} = -\frac{i\omega\varepsilon}{\alpha^4}\breve{E}_2^{\alpha} - \frac{i}{\omega}\partial_x\big[\frac{1}{\mu}(\partial_x \breve{E}_2^{\alpha} - \partial_y \breve{E}_1^{\alpha})\big] + \breve{J}_2\delta(z - L), \tag{3.4}$$

where ε and μ are taken at $(\alpha^2\boldsymbol{x}, z)$ and

$$\breve{\boldsymbol{J}}(\omega, \boldsymbol{x}) = \int \boldsymbol{J}(t, \boldsymbol{x}) e^{i\omega t} \mathrm{d}t\,.$$

The two other dependent variables $(\breve{E}_3^\alpha, \breve{H}_3^\alpha)$ are given by:

$$\breve{E}_3^\alpha = \frac{i\alpha^2}{\omega\varepsilon}(\partial_x \breve{H}_2^\alpha - \partial_y \breve{H}_1^\alpha) - \frac{i\alpha^4}{\omega\varepsilon}\breve{J}_3\delta(z-L), \tag{3.5}$$

$$\breve{H}_3^\alpha = -\frac{i\alpha^2}{\omega\mu}(\partial_x \breve{E}_2^\alpha - \partial_y \breve{E}_1^\alpha). \tag{3.6}$$

When the medium is homogeneous ($\varepsilon \equiv \varepsilon_0$ and $\mu \equiv \mu_0$), then there exist plane wave solutions that depend only on z and that satisfy:

$$\frac{\mathrm{d}}{\mathrm{d}z}\begin{bmatrix}\breve{E}_1^\alpha\\ \breve{H}_2^\alpha\\ \breve{E}_2^\alpha\\ \breve{H}_1^\alpha\end{bmatrix} = \frac{i\omega}{\alpha^4}\mathbf{M}\begin{bmatrix}\breve{E}_1^\alpha\\ \breve{H}_2^\alpha\\ \breve{E}_2^\alpha\\ \breve{H}_1^\alpha\end{bmatrix}, \quad \mathbf{M} = \begin{bmatrix}0 & \mu_0 & 0 & 0\\ \varepsilon_0 & 0 & 0 & 0\\ 0 & 0 & 0 & -\mu_0\\ 0 & 0 & -\varepsilon_0 & 0\end{bmatrix}.$$

The diagonalization of the 4×4 matrix $\mathbf{M}$ gives the general form of the plane wave solution

$$\begin{aligned}
\breve{E}_1^\alpha(\omega,z) &= \zeta_0^{\frac{1}{2}}\big(\breve{a}_1(\omega)e^{i\frac{\omega z}{c_0\alpha^4}} + \breve{b}_1(\omega)e^{-i\frac{\omega z}{c_0\alpha^4}}\big),\\
\breve{H}_2^\alpha(\omega,z) &= \zeta_0^{-\frac{1}{2}}\big(\breve{a}_1(\omega)e^{i\frac{\omega z}{c_0\alpha^4}} - \breve{b}_1(\omega)e^{-i\frac{\omega z}{c_0\alpha^4}}\big),\\
\breve{E}_2^\alpha(\omega,z) &= \zeta_0^{\frac{1}{2}}\big(\breve{a}_2(\omega)e^{i\frac{\omega z}{c_0\alpha^4}} + \breve{b}_2(\omega)e^{-i\frac{\omega z}{c_0\alpha^4}}\big),\\
\breve{H}_1^\alpha(\omega,z) &= \zeta_0^{-\frac{1}{2}}\big(-\breve{a}_2(\omega)e^{i\frac{\omega z}{c_0\alpha^4}} + \breve{b}_2(\omega)e^{-i\frac{\omega z}{c_0\alpha^4}}\big).
\end{aligned}$$

Here $c_0 = \mu_0^{-1/2}\varepsilon_0^{-1/2}$ and $\zeta_0 = \mu_0^{1/2}\varepsilon_0^{-1/2}$ are the homogeneous propagation speed and impedance. The modes $\breve{a}_j$, $j=1,2$, are right-going waves and the modes $\breve{b}_j$, $j=1,2$, are left-going waves.

When the medium is heterogeneous and described by the model (2.7-2.8), then we introduce the generalized right-going modes $\breve{a}_j^\alpha(\omega,\boldsymbol{x},z)$, $j=1,2$, and left-going modes $\breve{b}_j^\alpha(\omega,\boldsymbol{x},z)$, $j=1,2$, defined in the space $z>0$ by

$$\begin{aligned}
\breve{a}_1^\alpha(\omega,\boldsymbol{x},z) &= \frac{1}{2}\big(\zeta_0^{-\frac{1}{2}}\breve{E}_1^\alpha(\omega,\boldsymbol{x},z) + \zeta_0^{\frac{1}{2}}\breve{H}_2^\alpha(\omega,\boldsymbol{x},z)\Big)e^{-i\frac{\omega z}{c_0\alpha^4}},\\
\breve{b}_1^\alpha(\omega,\boldsymbol{x},z) &= \frac{1}{2}\big(\zeta_0^{-\frac{1}{2}}\breve{E}_1^\alpha(\omega,\boldsymbol{x},z) - \zeta_0^{\frac{1}{2}}\breve{H}_2^\alpha(\omega,\boldsymbol{x},z)\Big)e^{i\frac{\omega z}{c_0\alpha^4}},\\
\breve{a}_2^\alpha(\omega,\boldsymbol{x},z) &= \frac{1}{2}\Big(\zeta_0^{-\frac{1}{2}}\breve{E}_2^\alpha(\omega,\boldsymbol{x},z) - \zeta_0^{\frac{1}{2}}\breve{H}_1^\alpha(\omega,\boldsymbol{x},z)\Big)e^{-i\frac{\omega z}{c_0\alpha^4}},\\
\breve{b}_2^\alpha(\omega,\boldsymbol{x},z) &= \frac{1}{2}\Big(\zeta_0^{-\frac{1}{2}}\breve{E}_2^\alpha(\omega,\boldsymbol{x},z) + \zeta_0^{\frac{1}{2}}\breve{H}_1^\alpha(\omega,\boldsymbol{x},z)\Big)e^{i\frac{\omega z}{c_0\alpha^4}},
\end{aligned}$$

which gives the decomposition

$$\begin{aligned}
\breve{E}_1^\alpha(\omega,\boldsymbol{x},z) &= \zeta_0^{\frac{1}{2}}\big(\breve{a}_1^\alpha(\omega,\boldsymbol{x},z)e^{i\frac{\omega z}{c_0\alpha^4}} + \breve{b}_1^\alpha(\omega,\boldsymbol{x},z)e^{-i\frac{\omega z}{c_0\alpha^4}}\big),\\
\breve{H}_2^\alpha(\omega,\boldsymbol{x},z) &= \zeta_0^{-\frac{1}{2}}\big(\breve{a}_1^\alpha(\omega,\boldsymbol{x},z)e^{i\frac{\omega z}{c_0\alpha^4}} - \breve{b}_1^\alpha(\omega,\boldsymbol{x},z)e^{-i\frac{\omega z}{c_0\alpha^4}}\big),\\
\breve{E}_2^\alpha(\omega,\boldsymbol{x},z) &= \zeta_0^{\frac{1}{2}}\big(\breve{a}_2^\alpha(\omega,\boldsymbol{x},z)e^{i\frac{\omega z}{c_0\alpha^4}} + \breve{b}_2^\alpha(\omega,\boldsymbol{x},z)e^{-i\frac{\omega z}{c_0\alpha^4}}\big),\\
\breve{H}_1^\alpha(\omega,\boldsymbol{x},z) &= \zeta_0^{-\frac{1}{2}}\big(-\breve{a}_2^\alpha(\omega,\boldsymbol{x},z)e^{i\frac{\omega z}{c_0\alpha^4}} + \breve{b}_2^\alpha(\omega,\boldsymbol{x},z)e^{-i\frac{\omega z}{c_0\alpha^4}}\big).
\end{aligned}$$

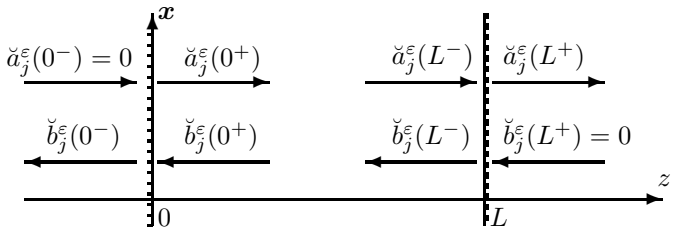

FIG. 3.1. *Boundary conditions for the modes in the presence of an interface at $z=0$, a random section $(0,L)$, and a source at $z=L$.*

In the space $z<0$ the modes are defined in terms of the propagation speed c_1 and impedance ζ_1 by

$$\begin{aligned}
\breve{a}_1^\alpha(\omega,\boldsymbol{x},z) &= \frac{1}{2}\big(\zeta_1^{-\frac{1}{2}}\breve{E}_1^\alpha(\omega,\boldsymbol{x},z)+\zeta_1^{\frac{1}{2}}\breve{H}_2^\alpha(\omega,\boldsymbol{x},z)\big)e^{-i\frac{\omega z}{c_1\alpha^4}},\\
\breve{b}_1^\alpha(\omega,\boldsymbol{x},z) &= \frac{1}{2}\big(\zeta_1^{-\frac{1}{2}}\breve{E}_1^\alpha(\omega,\boldsymbol{x},z)-\zeta_1^{\frac{1}{2}}\breve{H}_2^\alpha(\omega,\boldsymbol{x},z)\big)e^{i\frac{\omega z}{c_1\alpha^4}},\\
\breve{a}_2^\alpha(\omega,\boldsymbol{x},z) &= \frac{1}{2}\Big(\zeta_1^{-\frac{1}{2}}\breve{E}_2^\alpha(\omega,\boldsymbol{x},z)-\zeta_1^{\frac{1}{2}}\breve{H}_1^\alpha(\omega,\boldsymbol{x},z)\Big)e^{-i\frac{\omega z}{c_1\alpha^4}},\\
\breve{b}_2^\alpha(\omega,\boldsymbol{x},z) &= \frac{1}{2}\Big(\zeta_1^{-\frac{1}{2}}\breve{E}_2^\alpha(\omega,\boldsymbol{x},z)+\zeta_1^{\frac{1}{2}}\breve{H}_1^\alpha(\omega,\boldsymbol{x},z)\Big)e^{i\frac{\omega z}{c_1\alpha^4}}.
\end{aligned}$$

The radiation conditions at $+\infty$ and $-\infty$ implies that there is no left-going wave in the region $z>L$ and no right-going wave in the region $z<0$ (see Figure 3.1):

$$\breve{a}_j^\alpha(\omega,\boldsymbol{x},z=0^-)=0,\quad j=1,2, \tag{3.7}$$
$$\breve{b}_j^\alpha(\omega,\boldsymbol{x},z=L^+)=0,\quad j=1,2. \tag{3.8}$$

The jump conditions at the source plane $z=L$ are obtained by integrating (3.1-3.4) across $z=L$:

$$[\breve{E}_1^\alpha]_{L^-}^{L^+}=\frac{-i\alpha^2}{\omega\varepsilon_0}\partial_x\breve{J}_3,\quad [\breve{E}_2^\alpha]_{L^-}^{L^+}=\frac{-i\alpha^2}{\omega\varepsilon_0}\partial_y\breve{J}_3, \tag{3.9}$$
$$[\breve{H}_1^\alpha]_{L^-}^{L^+}=\breve{J}_2,\qquad [\breve{H}_2^\alpha]_{L^-}^{L^+}=-\breve{J}_1. \tag{3.10}$$

From the jump conditions (3.9-3.10) and the radiation conditions (3.8) we obtain:

$$\breve{b}_j^\alpha(\omega,\boldsymbol{x},z=L^-)=\breve{b}_{\mathrm{inc},j}^\alpha(\omega,\boldsymbol{x})e^{i\frac{\omega L}{c_0\alpha^4}},\quad j=1,2, \tag{3.11}$$
$$\breve{b}_{\mathrm{inc},1}^\alpha(\omega,\boldsymbol{x})=-\frac{\zeta_0^{\frac{1}{2}}}{2}\breve{J}_1(\omega,\boldsymbol{x})+\frac{i\alpha^2\zeta_0^{-\frac{1}{2}}}{2\omega\varepsilon_0}\partial_x\breve{J}_3(\omega,\boldsymbol{x}), \tag{3.12}$$
$$\breve{b}_{\mathrm{inc},2}^\alpha(\omega,\boldsymbol{x})=-\frac{\zeta_0^{\frac{1}{2}}}{2}\breve{J}_2(\omega,\boldsymbol{x})+\frac{i\alpha^2\zeta_0^{-\frac{1}{2}}}{2\omega\varepsilon_0}\partial_y\breve{J}_3(\omega,\boldsymbol{x}). \tag{3.13}$$

From the jump conditions (3.9-3.10) we obtain:

$$\breve{a}_j^\alpha(\omega,\boldsymbol{x},z=L^+)=\breve{a}_j^\alpha(\omega,\boldsymbol{x},z=L^-)+\breve{a}_{\mathrm{inc},j}^\alpha(\omega,\boldsymbol{x})e^{-i\frac{\omega L}{c_0\alpha^4}} \tag{3.14}$$

for $j = 1, 2$, where

$$\breve{a}^{\alpha}_{\mathrm{inc},1}(\omega, \boldsymbol{x}) = -\frac{\zeta_0^{\frac{1}{2}}}{2}\breve{J}_1(\omega, \boldsymbol{x}) - \frac{i\alpha^2\zeta_0^{-\frac{1}{2}}}{2\omega\varepsilon_0}\partial_x\breve{J}_3(\omega, \boldsymbol{x}), \tag{3.15}$$

$$\breve{a}^{\alpha}_{\mathrm{inc},2}(\omega, \boldsymbol{x}) = -\frac{\zeta_0^{\frac{1}{2}}}{2}\breve{J}_2(\omega, \boldsymbol{x}) - \frac{i\alpha^2\zeta_0^{-\frac{1}{2}}}{2\omega\varepsilon_0}\partial_y\breve{J}_3(\omega, \boldsymbol{x}). \tag{3.16}$$

Note that the terms $\breve{a}_{\mathrm{inc},j}$ are the wave fields generated by the source and that propagate to the right from the source. These fields propagate in the homogeneous right half-space $z > L$ and they never penetrate the random section. As we will see, they are concentrated in time around time 0.
By the continuity of the fields $(\breve{E}_j)_{j=1,2}$ and $(\breve{H}_j)_{j=1,2}$ across $z = 0$ and the radiation condition (3.7) at $-\infty$ we get:

$$\breve{a}^{\alpha}_j(\omega, \boldsymbol{x}, z = 0^+) = R_0\breve{b}^{\alpha}_j(\omega, \boldsymbol{x}, z = 0^+), \tag{3.17}$$

for $j = 1, 2$, and the transmitted left-going modes $\breve{b}^{\alpha}_j(\omega, \boldsymbol{x}, z = 0^-)$ are

$$\breve{b}^{\alpha}_j(\omega, \boldsymbol{x}, z = 0^-) = T_0\breve{b}^{\alpha}_j(\omega, \boldsymbol{x}, z = 0^+), \tag{3.18}$$

where R_0 and T_0 are the reflection and transmission coefficients of the interface at $z = 0$:

$$R_0 = \frac{\zeta_1 - \zeta_0}{\zeta_1 + \zeta_0}, \quad T_0 = \frac{2\sqrt{\zeta_1\zeta_0}}{\zeta_1 + \zeta_0}. \tag{3.19}$$

Let us introduce the four-dimensional vector

$$\breve{\boldsymbol{X}}^{\alpha}(\omega, \boldsymbol{x}, z) = \begin{bmatrix} \breve{a}^{\alpha}_1 \\ \breve{b}^{\alpha}_1 \\ \breve{a}^{\alpha}_2 \\ \breve{b}^{\alpha}_2 \end{bmatrix}(\omega, \boldsymbol{x}, z)e^{-i\frac{\omega L}{c_0\alpha^4}}. \tag{3.20}$$

By (3.1-3.4), the vector $\breve{\boldsymbol{X}}^{\alpha}$ satisfies in the region $z \in (0, L)$ the linear system

$$\frac{\mathrm{d}\breve{\boldsymbol{X}}^{\alpha}}{\mathrm{d}z} = \breve{\mathbf{A}}^{\alpha}(\omega, \boldsymbol{x}, z)\breve{\boldsymbol{X}}^{\alpha}, \tag{3.21}$$

$$\begin{aligned}\breve{\mathbf{A}}^{\alpha}(\omega, \boldsymbol{x}, z) = \breve{\mathbf{A}}^{0} + e^{2i\frac{\omega z}{\alpha^4 c_0}}\breve{\mathbf{A}}^{2} + e^{-2i\frac{\omega z}{\alpha^4 c_0}}\breve{\mathbf{A}}^{-2} + \frac{1}{\alpha}(n_\varepsilon + n_\mu)\big(\boldsymbol{x}, \frac{z}{\alpha^2}\big)\mathbf{B}^0 \\ + \frac{1}{\alpha}(n_\varepsilon - n_\mu)\big(\boldsymbol{x}, \frac{z}{\alpha^2}\big)\Big[e^{2i\frac{\omega z}{\alpha^4 c_0}}\mathbf{B}^2 + e^{-2i\frac{\omega z}{\alpha^4 c_0}}\mathbf{B}^{-2}\Big],\end{aligned} \tag{3.22}$$

and (3.11) and (3.17) give the two-point boundary conditions

$$\mathbf{K}^0\breve{\boldsymbol{X}}^{\alpha}(\omega, \boldsymbol{x}, 0) + \mathbf{K}^L\breve{\boldsymbol{X}}^{\alpha}(\omega, \boldsymbol{x}, L) = \breve{\boldsymbol{V}}^{\alpha}(\omega, \boldsymbol{x}). \tag{3.23}$$

The matrices $\breve{\mathbf{A}}^j$ and $\mathbf{B}^j$ are given in Appendix A and

$$\breve{\boldsymbol{V}}^{\alpha}(\omega, \boldsymbol{x}) = \begin{bmatrix} 0 \\ \breve{b}^{\alpha}_{\mathrm{inc},1}(\omega, \boldsymbol{x}) \\ 0 \\ \breve{b}^{\alpha}_{\mathrm{inc},2}(\omega, \boldsymbol{x}) \end{bmatrix}, \quad \mathbf{K}^0 = \begin{bmatrix} 1 & -R_0 & 0 & 0 \\ 0 & 0 & 0 & 0 \\ 0 & 0 & 1 & -R_0 \\ 0 & 0 & 0 & 0 \end{bmatrix}, \quad \mathbf{K}^L = \begin{bmatrix} 0 & 0 & 0 & 0 \\ 0 & 1 & 0 & 0 \\ 0 & 0 & 0 & 0 \\ 0 & 0 & 0 & 1 \end{bmatrix}. \tag{3.24}$$

In the expression (3.22) for $\breve{\mathbf{A}}^\alpha$ we have neglected terms of order α and smaller, and kept only the terms of order α^{-1} and 1. The mode decomposition has canceled the terms of order α^{-4} that are present in the original equations (3.1-3.4).

If the source is $\boldsymbol{x}$-independent and if the medium is homogeneous ($n_\varepsilon = n_\mu = 0$), then the solution of (3.21)-(3.23) is a constant vector which corresponds to a collection of left-going modes that propagate with the velocity c_0.

If the source is $\boldsymbol{x}$-dependent and/or the medium is heterogeneous, then transverse spatial effects and random effects have to be taken into account:
The matrices $\breve{\mathbf{A}}^j$ in (3.22) correspond to deterministic transverse spatial effects. They will give the diffraction term in the limit $\alpha \to 0$.
The matrices $\breve{\mathbf{B}}^j$ in (3.22) correspond to forward and backward scattering and coupling between modes due to the random heterogeneities of the medium. They are large, of order α^{-1}, but they vary rapidly at the scale α^2, and the driving processes have zero means and mixing properties. They will also give rise to effective terms of order one in the limit $\alpha \to 0$ through the application of a diffusion approximation theorem. The limit of $\breve{\boldsymbol{X}}^\alpha$ will be characterized by a stochastic partial differential equation driven by a Brownian field.

4. The random paraxial wave equations for the transmitted and reflected waves. In this section we state the main result of this paper, that we prove in the next two sections. Proposition 4.1 describes the transmitted wave in terms of a transmission operator solution of an Itô-Schrödinger equation.

PROPOSITION 4.1. *In the asymptotic regime $\alpha \to 0$, the transmitted wave is of the form:*

$$\begin{bmatrix} \boldsymbol{E} \\ \boldsymbol{H} \end{bmatrix} \left(t = \frac{L}{c_0} + \alpha^4 s, \alpha^2 \boldsymbol{x}, z = 0^- \right) \overset{\alpha \to 0}{\longrightarrow} \begin{bmatrix} \boldsymbol{E}^{(t)} \\ \boldsymbol{H}^{(t)} \end{bmatrix} (s, \boldsymbol{x}), \tag{4.1}$$

with

$$E_j^{(t)}(s, \boldsymbol{x}) = -\frac{\zeta_0^{\frac{1}{2}} \zeta_1^{\frac{1}{2}}}{4\pi} \iint \breve{\mathcal{T}}(\omega, \boldsymbol{x}, \boldsymbol{x}', L) \breve{J}_j(\omega, \boldsymbol{x}') \mathrm{d}\boldsymbol{x}' e^{-i\omega s} \mathrm{d}\omega, \quad j = 1, 2,$$

$E_3^{(t)} = 0$, $H_1^{(t)} = \zeta_1^{-1} E_2^{(t)}$, $H_2^{(t)} = -\zeta_1^{-1} E_1^{(t)}$, *and* $H_3^{(t)} = 0$. *The operator $\breve{\mathcal{T}}$ is the solution of the following Itô-Schrödinger diffusion model for $z \in (0, L)$*

$$\mathrm{d}\breve{\mathcal{T}}(\omega, \boldsymbol{x}, \boldsymbol{x}', z) = \frac{ic_0}{2\omega} \Delta_{\boldsymbol{x}'} \breve{\mathcal{T}}(\omega, \boldsymbol{x}, \boldsymbol{x}', z) \mathrm{d}z + \frac{i\omega}{2c_0} \breve{\mathcal{T}}(\omega, \boldsymbol{x}, \boldsymbol{x}', z) \circ \mathrm{d}B(\boldsymbol{x}', z), \tag{4.2}$$

with the initial conditions

$$\breve{\mathcal{T}}(\omega, \boldsymbol{x}, \boldsymbol{x}', z = 0) = T_0 \delta(\boldsymbol{x} - \boldsymbol{x}'). \tag{4.3}$$

Here $\Delta_{\boldsymbol{x}'} = \partial_{x'}^2 + \partial_{y'}^2$ is the transverse Laplacian, the symbol $\circ$ stands for the Stratonovich stochastic integral [22], and $B(\boldsymbol{x}, z)$ is a Brownian field with covariance

$$\mathbb{E}[B(\boldsymbol{x}, z) B(\boldsymbol{x}', z')] = \min\{z, z'\} C_0(\boldsymbol{x} - \boldsymbol{x}'), \tag{4.4}$$

with

$$C_0(\boldsymbol{x}) = \int_{-\infty}^{\infty} C(\boldsymbol{x}, z) \mathrm{d}z, \tag{4.5}$$
$$C(\boldsymbol{x}, z) = \mathbb{E}[(n_\varepsilon + n_\mu)(\boldsymbol{x}' + \boldsymbol{x}, z' + z)(n_\varepsilon + n_\mu)(\boldsymbol{x}', z')].$$

The time L/c_0 in (4.1) is the travel time from the source at $z = L$ to the interface $z = 0$ where the transmitted wave is observed. There is no other transmitted wave in the sense that for any time $t_0 \neq L/c_0$,

$$\begin{bmatrix} \boldsymbol{E} \\ \boldsymbol{H} \end{bmatrix} \left(t = t_0 + \alpha^4 s, \alpha^2 \boldsymbol{x}, z = 0^-\right) \overset{\alpha \to 0}{\longrightarrow} \begin{bmatrix} \boldsymbol{0} \\ \boldsymbol{0} \end{bmatrix}.$$

In [10] the existence and uniqueness has been established for the random process

$$V(\omega, \boldsymbol{x}, z) = {T_0}^{-1} \int \breve{T}(\omega, \boldsymbol{x}, \boldsymbol{x}', z)\phi(\boldsymbol{x}')\mathrm{d}\boldsymbol{x}',$$

for any test function ϕ with unit $L^2(\mathbb{R}^2)$-norm. It is shown that the process $V(\omega, \boldsymbol{x}, z)$ is a continuous Markov diffusion process on the unit ball of $L^2(\mathbb{R}^2)$. The moment equations moreover satisfy a closed system at each order [20], which allows for explicit calculations of the mean intensity and the autocorrelation function [24].

The covariance of the effective Brownian field B depends on the two-point statistics of $n_\varepsilon + n_\mu$. Considering the model (2.7-2.8) for the medium parameters, this means that the effective Brownian field is determined by the fluctuations of the local propagation speed

$$c(z, \boldsymbol{x}) = \sqrt{\mu\varepsilon} = c_0\big[1 + \alpha^3 \frac{n_\mu + n_\varepsilon}{2}(z, \boldsymbol{x}) + O(\alpha^6)\big],$$

but not by the fluctuations of the local impedance

$$\zeta(z, \boldsymbol{x}) = \sqrt{\mu/\varepsilon} = \zeta_0\big[1 + \alpha^3 \frac{n_\mu - n_\varepsilon}{2}(z, \boldsymbol{x}) + O(\alpha^6)\big].$$

We can explain this by saying that the fluctuations of the local impedance are responsible for backscattering, which is negligible in the scaled regime considered in this paper. Therefore, the detailed statistical information on the fluctuations of the impedance is lost. However, the fluctuations of the local propagation speed are responsible for wave front distortion, and that is why they appear in the formulation of the random paraxial wave equation.

Proposition 4.1 shows that, although the medium fluctuations can be statistically isotropic, the strongly anisotropic scaling corresponding to beam propagation leads to an approximation of the wave process with a noise model which is δ-correlated in the z-direction but exhibits correlation in the lateral directions. In the case of turbulent atmosphere [31], the power spectral density of the fluctuations (proportional to the Fourier transform of the autocorrelation function) is of the form (for $\boldsymbol{k} = (k, \boldsymbol{\kappa})$, $\boldsymbol{\kappa} \in \mathbb{R}^2$)

$$\widehat{C}(\boldsymbol{k}) = \iint C(z, \boldsymbol{x}) e^{-ikz - i\boldsymbol{\kappa}\cdot\boldsymbol{x}} \mathrm{d}z\mathrm{d}\boldsymbol{x} \sim |\boldsymbol{k}|^{-3-2H} \text{ for } |\boldsymbol{k}| \in \left(\frac{2\pi}{L_0}, \frac{2\pi}{l_0}\right),$$

where $H = 1/3$, l_0 (resp. L_0) is the inner scale (resp. outer scale) of the turbulence. This corresponds to a spatial structure function

$$\begin{aligned} D(\boldsymbol{x}, z) &:= \mathbb{E}\big[\left((n_\varepsilon + n_\mu)(\boldsymbol{x}', z') - (n_\varepsilon + n_\mu)(\boldsymbol{x}' + \boldsymbol{x}, z' + z)\right)^2\big] \\ &\propto (|\boldsymbol{x}|^2 + z^2)^H \text{ for } \sqrt{|\boldsymbol{x}|^2 + z^2} \in (l_0, L_0). \end{aligned}$$

The lateral power spectral density of the white-noise model can be obtained from (4.5) and it is given by

$$\widehat{C}_0(\boldsymbol{\kappa}) = \int C_0(\boldsymbol{x}) e^{-i\boldsymbol{\kappa}\cdot\boldsymbol{x}} \mathrm{d}\boldsymbol{x} \sim |\boldsymbol{\kappa}|^{-2-2(H+\frac{1}{2})} \text{ for } |\boldsymbol{\kappa}| \in \left(\frac{2\pi}{L_0}, \frac{2\pi}{l_0}\right),$$

giving rise to the modified spectral exponent $H + 1/2$ in the lateral direction [16].

We now describe the reflected field.

PROPOSITION 4.2. *In the asymptotic regime $\alpha \to 0$, the reflected wave is of the form:*

$$\begin{bmatrix} \boldsymbol{E} \\ \boldsymbol{H} \end{bmatrix} \left(t = \frac{2L}{c_0} + \alpha^4 s, \alpha^2 \boldsymbol{x}, z = L^+\right) \overset{\alpha\to 0}{\longrightarrow} \begin{bmatrix} \boldsymbol{E}^{(r)} \\ \boldsymbol{H}^{(r)} \end{bmatrix} (s, \boldsymbol{x}), \tag{4.6}$$

with

$$E_j^{(r)}(s, \boldsymbol{x}) = -\frac{\zeta_0}{4\pi} \iint \breve{\mathcal{R}}(\omega, \boldsymbol{x}, \boldsymbol{x}', L) \breve{J}_j(\omega, \boldsymbol{x}') \mathrm{d}\boldsymbol{x}' e^{-i\omega s} \mathrm{d}\omega, \quad j = 1, 2,$$

$E_3^{(r)} = 0$ $H_1^{(r)} = -\zeta_0^{-1} E_2^{(r)}$, $H_2^{(r)} = \zeta_0^{-1} E_1^{(r)}$, *and* $H_3^{(r)} = 0$. *The operator $\breve{\mathcal{R}}$ is the solution of the following Itô-Schrödinger diffusion model*

$$\begin{aligned} \mathrm{d}\breve{\mathcal{R}}(\omega, \boldsymbol{x}, \boldsymbol{x}', z) = {} & \frac{ic_0}{2\omega} \big(\Delta_{\boldsymbol{x}} + \Delta_{\boldsymbol{x}'}\big) \breve{\mathcal{R}}(\omega, \boldsymbol{x}, \boldsymbol{x}', z) \mathrm{d}z \\ & + \frac{i\omega}{2c_0} \breve{\mathcal{R}}(\omega, \boldsymbol{x}, \boldsymbol{x}', z) \circ \big(\mathrm{d}B(\boldsymbol{x}, z) + \mathrm{d}B(\boldsymbol{x}', z)\big), \end{aligned} \tag{4.7}$$

with the initial conditions

$$\breve{\mathcal{R}}(\omega, \boldsymbol{x}, \boldsymbol{x}', z = 0) = R_0 \delta(\boldsymbol{x} - \boldsymbol{x}'). \tag{4.8}$$

The time $2L/c_0$ in (4.6) is the travel time for a round trip from the surface $z = L$ to the interface $z = 0$. At time 0 we can also observe the wave field that is emitted by the source and propagating to the right into the homogeneous half-space (L, ∞):

$$\begin{bmatrix} \boldsymbol{E} \\ \boldsymbol{H} \end{bmatrix} \left(t = \alpha^4 s, \alpha^2 \boldsymbol{x}, z = L^+\right) \overset{\alpha\to 0}{\longrightarrow} \begin{bmatrix} \boldsymbol{E}^{(o)} \\ \boldsymbol{H}^{(o)} \end{bmatrix} (s, \boldsymbol{x}),$$

with

$$E_j^{(o)}(s, \boldsymbol{x}) = -\frac{\zeta_0}{2} J_j(s, \boldsymbol{x}), \quad j = 1, 2, \qquad E_3^{(o)}(s, \boldsymbol{x}) = 0,$$

$H_1^{(o)} = -\zeta_0^{-1} E_2^{(o)}$, $H_2^{(o)} = \zeta_0^{-1} E_1^{(o)}$, and $H_3^{(o)} = 0$.

There is no other reflected wave, in the sense that for any $t_0 \notin \{0, 2L/c_0\}$,

$$\begin{bmatrix} \boldsymbol{E} \\ \boldsymbol{H} \end{bmatrix} \left(t = t_0 + \alpha^4 s, \alpha^2 \boldsymbol{x}, z = L^+\right) \overset{\alpha\to 0}{\longrightarrow} \begin{bmatrix} \boldsymbol{0} \\ \boldsymbol{0} \end{bmatrix}.$$

If there is no impedance contrast at the interface at $z = 0$, that is, if $\zeta_1 = \zeta_0$, then $R_0 = 0$ and the reflection operator $\breve{\mathcal{R}}$ vanish. This shows that no wave is reflected in this case. This result is the rigorous proof that the forward-scattering approximation is valid in the scaled regime considered in the paper, and that the wave field is then described by the paraxial white-noise model (4.2).

It is important to note that the stochastic partial differential equation (4.7) is driven by a unique Brownian field B. This comes from the fact that the wave propagates in the same medium when traveling from $z = L$ to the interface $z = 0$ and when traveling back from $z = 0$ to $z = L$. In particular this fact is responsible for the enhanced backscattering phenomenon that we analyze in Section 7.1.

The proofs of Propositions 4.1-4.2 that we will present in the next two sections give the convergence of the joint process consisting of the transmitted and reflected wave fields, with the *same* Brownian field used in the Itô-Schrödinger models (4.2) and (4.7). Moreover, the Itô-Schrödinger model preserves the L^2-norm and we have the identity $R_0^2+T_0^2 = 1$. As a result we obtain the conservation of energy of the reflection-transmission problem, in the sense that the sum of the energies of the transmitted wave and of the reflected wave is equal to the energy of the incident wave.

5. The derivation of the paraxial wave equation.

5.1. The homogeneous case. Let us assume in this section that the medium is homogeneous: $n_\varepsilon = n_\mu = 0$. We transform the two-point boundary value problem (3.21)-(3.23) into an initial value problem. This is done by an invariant imbedding step in which we introduce transmission and reflection matrices. First, we define the lateral Fourier modes for $\boldsymbol{\kappa} = (\kappa_x, \kappa_y) \in \mathbb{R}^2$:

$$\widehat{a}_j^\alpha(\omega, \boldsymbol{\kappa}, z) = \int \breve{a}_j^\alpha(\omega, \boldsymbol{x}, z) e^{-i\boldsymbol{\kappa}\cdot\boldsymbol{x}} \mathrm{d}\boldsymbol{x}, \qquad \widehat{b}_j^\alpha(\omega, \boldsymbol{\kappa}, z) = \int \breve{b}_j^\alpha(\omega, \boldsymbol{x}, z) e^{-i\boldsymbol{\kappa}\cdot\boldsymbol{x}} \mathrm{d}\boldsymbol{x}.$$

The reflected wave is characterized by $\widehat{a}_j^\alpha(\omega, \boldsymbol{\kappa}, z = L^+)$, $j = 1, 2$, and the transmitted wave by $\widehat{b}_j^\alpha(\omega, \boldsymbol{\kappa}, z = 0^-)$, $j = 1, 2$. The parameters ω and $\boldsymbol{\kappa}$ are frozen in the problem, so we shall not write explicitly the $(\omega, \boldsymbol{\kappa})$-dependence of the vectors and matrices. The vector $\widehat{\boldsymbol{X}}^\alpha(z)$ defined as in (3.20) with the Fourier modes $\widehat{a}_j^\alpha$ and $\widehat{b}_j^\alpha$ is solution of the two-point boundary value problem:

$$\frac{\mathrm{d}\widehat{\boldsymbol{X}}^\alpha}{\mathrm{d}z} = \widehat{\mathbf{A}}^\alpha(z)\widehat{\boldsymbol{X}}^\alpha, \qquad \mathbf{K}^0\widehat{\boldsymbol{X}}^\alpha(0) + \mathbf{K}^L\widehat{\boldsymbol{X}}^\alpha(L) = \widehat{\boldsymbol{V}}^\alpha,$$

with the 4×4 matrix $\widehat{\mathbf{A}}^\alpha(z)$ given by

$$\widehat{\mathbf{A}}^\alpha(z) = \widehat{\mathbf{A}}^0 + e^{2i\frac{\omega z}{\alpha^4 c_0}}\widehat{\mathbf{A}}^2 + e^{-2i\frac{\omega z}{\alpha^4 c_0}}\widehat{\mathbf{A}}^{-2},$$

$\widehat{\mathbf{A}}^j$ are given in Appendix A, $\mathbf{K}^0$ and $\mathbf{K}^L$ are given by (3.24) and

$$\widehat{\boldsymbol{V}}^\alpha = \begin{bmatrix} 0 \\ \widehat{b}^\alpha_{\mathrm{inc},1} \\ 0 \\ \widehat{b}^\alpha_{\mathrm{inc},2} \end{bmatrix}, \qquad \widehat{b}^\alpha_{\mathrm{inc},j}(\omega, \boldsymbol{\kappa}) = \int \breve{b}^\alpha_{\mathrm{inc},j}(\omega, \boldsymbol{x}) e^{-i\boldsymbol{\kappa}\cdot\boldsymbol{x}} \mathrm{d}\boldsymbol{x}.$$

By applying Proposition B.1, we get that

$$\widehat{a}_j^\alpha(z = L^-) = [\widehat{\mathbf{R}}^\alpha(L)\widehat{\boldsymbol{V}}^\alpha]_{2j-1} e^{i\frac{\omega L}{c_0\alpha^4}}, \tag{5.1}$$

$$\widehat{b}_j^\alpha(z = 0^+) = [\widehat{\mathbf{T}}^\alpha(L)\widehat{\boldsymbol{V}}^\alpha]_{2j} e^{i\frac{\omega L}{c_0\alpha^4}}, \tag{5.2}$$

for $j = 1, 2$, where the reflection and transmission matrices $\widehat{\mathbf{R}}^\alpha$ and $\widehat{\mathbf{T}}^\alpha$ are solution of the initial value problem

$$\frac{\mathrm{d}\widehat{\mathbf{R}}^\alpha}{\mathrm{d}z} = (\mathbf{I} - \widehat{\mathbf{R}}^\alpha \mathbf{K}^L)\widehat{\mathbf{A}}^\alpha(z)\widehat{\mathbf{R}}^\alpha, \qquad \widehat{\mathbf{R}}^\alpha(0) = \mathbf{K}, \tag{5.3}$$

$$\frac{\mathrm{d}\widehat{\mathbf{T}}^\alpha}{\mathrm{d}z} = -\widehat{\mathbf{T}}^\alpha \mathbf{K}^L \widehat{\mathbf{A}}^\alpha(z)\widehat{\mathbf{R}}^\alpha, \qquad \widehat{\mathbf{T}}^\alpha(0) = \mathbf{K}, \tag{5.4}$$

where $\mathbf{I}$ the 4×4 identity matrix and

$$\mathbf{K} = \left(\mathbf{K}^0 + \mathbf{K}^L\right)^{-1} = \begin{bmatrix} 1 & R_0 & 0 & 0 \\ 0 & 1 & 0 & 0 \\ 0 & 0 & 1 & R_0 \\ 0 & 0 & 0 & 1 \end{bmatrix}. \tag{5.5}$$

Therefore, using (3.18) and (3.14), the reflected and transmitted modes are given by

$$\widehat{a}_j^\alpha(z = L^+) = [\widehat{\mathbf{R}}^\alpha(L)\widehat{\boldsymbol{V}}^\alpha]_{2j-1} e^{i\frac{\omega L}{c_0 \alpha^4}} + \widehat{a}_{\mathrm{inc},j}^\alpha e^{-i\frac{\omega L}{c_0 \alpha^4}}, \tag{5.6}$$

$$\widehat{b}_j^\alpha(z = 0^-) = T_0[\widehat{\mathbf{T}}^\alpha(L)\widehat{\boldsymbol{V}}^\alpha]_{2j} e^{i\frac{\omega L}{c_0 \alpha^4}}, \tag{5.7}$$

for $j = 1, 2$. Note that the second term $\widehat{a}_{\mathrm{inc},j}^\alpha$ in the expression of $\widehat{a}_j^\alpha(z = L^+)$ is actually the wave that is emitted by the source and traveling to the right.

Then we can apply a standard averaging theorem [19, Chapter 6] which gives the asymptotic behavior of the reflection and transmission matrices:

$$\frac{\mathrm{d}\widehat{\mathbf{R}}}{\mathrm{d}z} = (\mathbf{I} - \widehat{\mathbf{R}}\mathbf{K}^L)\widehat{\mathbf{A}}^0\widehat{\mathbf{R}}, \qquad \widehat{\mathbf{R}}(0) = \mathbf{K}, \tag{5.8}$$

$$\frac{\mathrm{d}\widehat{\mathbf{T}}}{\mathrm{d}z} = -\widehat{\mathbf{T}}\mathbf{K}^L\widehat{\mathbf{A}}^0\widehat{\mathbf{R}}, \qquad \widehat{\mathbf{T}}(0) = \mathbf{K}. \tag{5.9}$$

We also have

$$\lim_{\alpha \to 0} \widehat{\boldsymbol{V}}^\alpha = \widehat{\boldsymbol{V}} := \begin{bmatrix} 0 \\ \widehat{b}_{\mathrm{inc},1} \\ 0 \\ \widehat{b}_{\mathrm{inc},2} \end{bmatrix} = -\frac{\zeta_0^{\frac{1}{2}}}{2} \begin{bmatrix} 0 \\ \widehat{J}_1 \\ 0 \\ \widehat{J}_2 \end{bmatrix}, \tag{5.10}$$

$$\lim_{\alpha \to 0} \begin{bmatrix} \widehat{a}_{\mathrm{inc},1}^\alpha \\ \widehat{a}_{\mathrm{inc},2}^\alpha \end{bmatrix} = \begin{bmatrix} \widehat{b}_{\mathrm{inc},1} \\ \widehat{b}_{\mathrm{inc},2} \end{bmatrix} = -\frac{\zeta_0^{\frac{1}{2}}}{2} \begin{bmatrix} \widehat{J}_1 \\ \widehat{J}_2 \end{bmatrix}. \tag{5.11}$$

The solution of (5.8) is the matrix:

$$\widehat{\mathbf{R}}(z) = \begin{bmatrix} \widetilde{R}(z) & \widehat{R}(z) & 0 & 0 \\ 0 & 1 & 0 & 0 \\ 0 & 0 & \widetilde{R}(z) & \widehat{R}(z) \\ 0 & 0 & 0 & 1 \end{bmatrix},$$

where $\widetilde{R}$ and $\widehat{R}$ are the solutions of

$$\frac{\mathrm{d}\widetilde{R}}{\mathrm{d}z} = \widehat{A}_{11}^0 \widetilde{R}, \qquad \widetilde{R}(0) = 1,$$

$$\frac{\mathrm{d}\widehat{R}}{\mathrm{d}z} = \widehat{A}_{11}^0 \widehat{R} - \widehat{R}\widehat{A}_{22}^0, \qquad \widehat{R}(0) = R_0.$$

Therefore

$$\lim_{\alpha\to 0}[\widehat{\mathbf{R}}^\alpha(L)\widehat{\boldsymbol{V}}^\alpha]_{2j-1} = [\widehat{\mathbf{R}}(L)\widehat{\boldsymbol{V}}]_{2j-1} = -\frac{\zeta_0^{\frac{1}{2}}}{2}\widehat{R}(L)\widehat{J}_j, \tag{5.12}$$

for $j = 1, 2$. The solution of (5.9) is the matrix:

$$\widehat{\mathbf{T}}(z) = \begin{bmatrix} 1 & \widetilde{T}(z) & 0 & 0 \\ 0 & \widehat{T}(z) & 0 & 0 \\ 0 & 0 & 1 & \widetilde{T}(z) \\ 0 & 0 & 0 & \widehat{T}(z) \end{bmatrix},$$

where $\widetilde{T}$ and $\widehat{T}$ are the solutions of

$$\begin{aligned} \frac{\mathrm{d}\widetilde{T}}{\mathrm{d}z} &= -\widetilde{T}\widehat{A}^0_{22}, \qquad & \widetilde{T}(0) &= R_0, \\ \frac{\mathrm{d}\widehat{T}}{\mathrm{d}z} &= -\widehat{T}\widehat{A}^0_{22}, \qquad & \widehat{T}(0) &= 1. \end{aligned}$$

Therefore

$$\lim_{\alpha\to 0}[\widehat{\mathbf{T}}^\alpha(L)\widehat{\boldsymbol{V}}^\alpha]_{2j} = [\widehat{\mathbf{T}}(L)\widehat{\boldsymbol{V}}]_{2j} = -\frac{\zeta_0^{\frac{1}{2}}}{2}\widehat{T}(L)\widehat{J}_j, \tag{5.13}$$

for $j = 1, 2$.

The transmitted wave field at $z = 0^-$ is

$$E_j(t, \alpha^2\boldsymbol{x}, 0^-) = \frac{\zeta_1^{\frac{1}{2}}}{(2\pi)^3}\iint \widehat{b}^\alpha_j(\omega, \boldsymbol{\kappa}, 0^-)e^{i\boldsymbol{\kappa}\cdot\boldsymbol{x}}\mathrm{d}\boldsymbol{\kappa}e^{-i\frac{\omega}{\alpha^4}t}\mathrm{d}\omega,$$

and $H_j = \zeta_1 E_j$, $j = 1, 2$, while the components E_3 and H_3 are obtained through (3.5-3.6). Substituting (5.7) into this integral representation gives

$$E_j(t, \alpha^2\boldsymbol{x}, 0^-) = \frac{\zeta_1^{\frac{1}{2}}T_0}{(2\pi)^3}\iint \big[\widehat{\mathbf{T}}^\alpha(\omega, \boldsymbol{\kappa}, L)\widehat{\boldsymbol{V}}^\alpha(\omega, \boldsymbol{\kappa})\big]_{2j}e^{i\boldsymbol{\kappa}\cdot\boldsymbol{x}}\mathrm{d}\boldsymbol{\kappa}e^{i\frac{\omega}{\alpha^4}(\frac{L}{c_0}-t)}\mathrm{d}\omega.$$

By (5.13), we obtain

$$\lim_{\alpha\to 0} E_j\Big(\frac{L}{c_0} + \alpha^4 s, \alpha^2\boldsymbol{x}, 0^-\Big) = -\frac{\zeta_0^{\frac{1}{2}}\zeta_1^{\frac{1}{2}}T_0}{2(2\pi)^3}\iint \widehat{T}(\omega, \boldsymbol{\kappa}, L)\widehat{J}_j(\omega, \boldsymbol{\kappa})e^{i\boldsymbol{\kappa}\cdot\boldsymbol{x}}\mathrm{d}\boldsymbol{\kappa}e^{-i\omega s}\mathrm{d}\omega.$$

By taking an inverse Fourier transform in $\boldsymbol{\kappa}$, we obtain the result of the proposition (without the Brownian field). The kernel of the operator $\breve{\mathcal{T}}$ is here of the form

$$\breve{\mathcal{T}}(\omega, \boldsymbol{x}, \boldsymbol{x}', z) = \frac{T_0}{(2\pi)^2}\int \widehat{T}(\omega, \boldsymbol{\kappa}, z)e^{i\boldsymbol{\kappa}\cdot(\boldsymbol{x}-\boldsymbol{x}')}\mathrm{d}\boldsymbol{\kappa}. \tag{5.14}$$

The reflected wave field at $z = L^+$ is

$$E_j(t, \alpha^2\boldsymbol{x}, L^+) = \frac{\zeta_0^{\frac{1}{2}}}{(2\pi)^3}\iint \widehat{a}^\alpha_j(\omega, \boldsymbol{\kappa}, L^+)e^{i\boldsymbol{\kappa}\cdot\boldsymbol{x}}\mathrm{d}\boldsymbol{\kappa}e^{i\frac{\omega}{\alpha^4}(\frac{L}{c_0}-t)}\mathrm{d}\omega.$$

Substituting (5.6) into this integral representation gives

$$E_j(t,\alpha^2\boldsymbol{x},L^+)=\frac{\zeta_0^{\frac12}}{(2\pi)^3}\iint\big[\widehat{\mathbf{R}}^\alpha(\omega,\boldsymbol{\kappa},L)\widehat{\boldsymbol{V}}^\alpha(\omega,\boldsymbol{\kappa})\big]_{2j-1}e^{i\boldsymbol{\kappa}\cdot\boldsymbol{x}}\mathrm{d}\boldsymbol{\kappa}e^{i\frac{\omega}{\alpha^4}(\frac{2L}{c_0}-t)}\mathrm{d}\omega$$
$$+\frac{\zeta_0^{\frac12}}{(2\pi)^3}\iint\widehat{a}^\alpha_{\mathrm{inc},j}(\omega,\boldsymbol{\kappa})e^{i\boldsymbol{\kappa}\cdot\boldsymbol{x}}\mathrm{d}\boldsymbol{\kappa}e^{-i\frac{\omega}{\alpha^4}t}\mathrm{d}\omega.$$

By (5.11), we obtain

$$\lim_{\alpha\to0}E_j\big(\alpha^4s,\alpha^2\boldsymbol{x},L^+\big)=-\frac{\zeta_0}{2(2\pi)^3}\iint\widehat{J}_j(\omega,\boldsymbol{\kappa})e^{i\boldsymbol{\kappa}\cdot\boldsymbol{x}}\mathrm{d}\boldsymbol{\kappa}e^{-i\omega s}\mathrm{d}\omega,$$

which is the wave that is emitted to the right by the source. By (5.12),

$$\lim_{\alpha\to0}E_j\Big(\frac{2L}{c_0}+\alpha^4s,\alpha^2\boldsymbol{x},L^+\Big)=-\frac{\zeta_0}{2(2\pi)^3}\iint\widehat{R}(\omega,\boldsymbol{\kappa},L)\widehat{J}_j(\omega,\boldsymbol{\kappa})e^{i\boldsymbol{\kappa}\cdot\boldsymbol{x}}\mathrm{d}\boldsymbol{\kappa}e^{-i\omega s}\mathrm{d}\omega,$$

which is the wave emitted to the left by the source and reflected by the random section. By taking an inverse Fourier transform in $\boldsymbol{\kappa}$, we obtain the result of the proposition. The kernel of the operator $\breve{\mathcal{R}}$ is here of the form

$$\breve{\mathcal{R}}(\omega,\boldsymbol{x},\boldsymbol{x}',z)=\frac{1}{(2\pi)^2}\int\widehat{R}(\omega,\boldsymbol{\kappa},z)e^{i\boldsymbol{\kappa}\cdot(\boldsymbol{x}-\boldsymbol{x}')}\mathrm{d}\boldsymbol{\kappa}.\tag{5.15}$$

5.2. The random case. We transform the two-point boundary value problem (3.21)-(3.23) into an initial value problem. This is very important in the random case so as to deal with quantities that are adapted to the filtration of the random driving processes n_ε and n_μ. This transformation is done by an invariant imbedding step in which we introduce transmission and reflection operators. The algebra is more complicated than in the homogeneous case since the random medium fluctuations involve coupling not only between the four modes (as in the homogeneous case) but also between different $\boldsymbol{\kappa}$-modes. That is why we need to introduce matrix operators. The vector $\widehat{\boldsymbol{X}}^\alpha$ defined as in (3.20) is solution of the two-point boundary value problem:

$$\frac{\mathrm{d}\widehat{\boldsymbol{X}}^\alpha}{\mathrm{d}z}=\widehat{\boldsymbol{\mathcal{A}}}^\alpha(z)\widehat{\boldsymbol{X}}^\alpha,\qquad\mathbf{K}^0\widehat{\boldsymbol{X}}^\alpha(0)+\mathbf{K}^L\widehat{\boldsymbol{X}}^\alpha(L)=\widehat{\boldsymbol{V}}^\alpha.$$

Here $\widehat{\boldsymbol{\mathcal{A}}}^\alpha(z)$ is the matrix operator acting on four-dimensional vector fields $\widehat{\boldsymbol{Y}}(\boldsymbol{\kappa})$ as

$$[\widehat{\boldsymbol{\mathcal{A}}}^\alpha(z)\widehat{\boldsymbol{Y}}](\boldsymbol{\kappa})=\int\widehat{\boldsymbol{\mathcal{A}}}^\alpha(\boldsymbol{\kappa},\boldsymbol{\kappa}',z)\widehat{\boldsymbol{Y}}(\boldsymbol{\kappa}')\mathrm{d}\boldsymbol{\kappa}',$$

with the kernel

$$\widehat{\boldsymbol{\mathcal{A}}}^\alpha(\boldsymbol{\kappa},\boldsymbol{\kappa}',z)=\delta(\boldsymbol{\kappa}-\boldsymbol{\kappa}')\Big[\widehat{\mathbf{A}}^0+e^{2i\frac{\omega z}{\alpha^4c_0}}\widehat{\mathbf{A}}^2+e^{-2i\frac{\omega z}{\alpha^4c_0}}\widehat{\mathbf{A}}^{-2}\Big]$$
$$+\frac{1}{\alpha}\frac{1}{(2\pi)^2}(\widehat{n}_\varepsilon-\widehat{n}_\mu)\big(\boldsymbol{\kappa}-\boldsymbol{\kappa}',\frac{z}{\alpha^2}\big)\Big[e^{2i\frac{\omega z}{\alpha^4c_0}}\mathbf{B}^2+e^{-2i\frac{\omega z}{\alpha^4c_0}}\mathbf{B}^{-2}\Big]$$
$$+\frac{1}{\alpha}\frac{1}{(2\pi)^2}(\widehat{n}_\varepsilon+\widehat{n}_\mu)\big(\boldsymbol{\kappa}-\boldsymbol{\kappa}',\frac{z}{\alpha^2}\big)\mathbf{B}^0.\tag{5.16}$$

The matrices $\widehat{\mathbf{A}}^j$ and $\mathbf{B}^j$ are given in Appendix A. By applying Proposition B.1, we get that the reflected and transmitted modes are given by

$$\widehat{a}_j^\alpha(z=L^+) = [\widehat{\boldsymbol{\mathcal{R}}}^\alpha(L)\widehat{\boldsymbol{V}}^\alpha]_{2j-1} e^{i\frac{\omega L}{c_0\alpha^4}} + \widehat{a}^\alpha_{\mathrm{inc},j} e^{-i\frac{\omega L}{c_0\alpha^4}},$$
$$\widehat{b}_j^\alpha(z=0^-) = T_0[\widehat{\boldsymbol{\mathcal{T}}}^\alpha(L)\widehat{\boldsymbol{V}}^\alpha]_{2j} e^{i\frac{\omega L}{c_0\alpha^4}},$$

for $j=1,2$, where the reflection and transmission matrix operators are solution of the initial value problem

$$\frac{\mathrm{d}\widehat{\boldsymbol{\mathcal{R}}}^\alpha}{\mathrm{d}z} = (\widehat{\boldsymbol{\mathcal{I}}} - \widehat{\boldsymbol{\mathcal{R}}}^\alpha \widehat{\boldsymbol{\mathcal{K}}}^L)\widehat{\boldsymbol{\mathcal{A}}}^\alpha(z)\widehat{\boldsymbol{\mathcal{R}}}^\alpha, \qquad \widehat{\boldsymbol{\mathcal{R}}}^\alpha(0) = \widehat{\boldsymbol{\mathcal{K}}},$$
$$\frac{\mathrm{d}\widehat{\boldsymbol{\mathcal{T}}}^\alpha}{\mathrm{d}z} = -\widehat{\boldsymbol{\mathcal{T}}}^\alpha \widehat{\boldsymbol{\mathcal{K}}}^L \widehat{\boldsymbol{\mathcal{A}}}^\alpha(z)\widehat{\boldsymbol{\mathcal{R}}}^\alpha, \qquad \widehat{\boldsymbol{\mathcal{T}}}^\alpha(0) = \widehat{\boldsymbol{\mathcal{K}}}.$$

Here the kernels of $\widehat{\boldsymbol{\mathcal{I}}}$, $\widehat{\boldsymbol{\mathcal{K}}}$, and $\widehat{\boldsymbol{\mathcal{K}}}^L$ are

$$\widehat{\boldsymbol{\mathcal{I}}}(\boldsymbol{\kappa},\boldsymbol{\kappa}') = \delta(\boldsymbol{\kappa}-\boldsymbol{\kappa}')\mathbf{I}, \qquad \widehat{\boldsymbol{\mathcal{K}}}(\boldsymbol{\kappa},\boldsymbol{\kappa}') = \delta(\boldsymbol{\kappa}-\boldsymbol{\kappa}')\mathbf{K}, \qquad \widehat{\boldsymbol{\mathcal{K}}}^L(\boldsymbol{\kappa},\boldsymbol{\kappa}') = \delta(\boldsymbol{\kappa}-\boldsymbol{\kappa}')\mathbf{K}^L,$$

and $\mathbf{K}$ is the 4×4 matrix defined by (5.5).

Explicitly, the reflected and transmitted wave components are, for $j=1,2$:

$$E_j(t,\alpha^2\boldsymbol{x},L^+) = \frac{\zeta_0^{\frac12}}{(2\pi)^3}\iint \widehat{a}^\alpha_{\mathrm{inc},j}(\omega,\boldsymbol{\kappa}) e^{i\boldsymbol{\kappa}\cdot\boldsymbol{x}}\mathrm{d}\boldsymbol{\kappa} e^{-i\frac{\omega}{\alpha^4}t}\mathrm{d}\omega$$
$$+\frac{\zeta_0^{\frac12}}{(2\pi)^3}\iint \sum_{k=1}^2 \widehat{\mathcal{R}}^\alpha_{2j-1,2k}(\omega,\boldsymbol{\kappa},\boldsymbol{\kappa}',L)\widehat{b}^\alpha_{\mathrm{inc},k}(\omega,\boldsymbol{\kappa}') e^{i\boldsymbol{\kappa}\cdot\boldsymbol{x}}\mathrm{d}\boldsymbol{\kappa}'\mathrm{d}\boldsymbol{\kappa} e^{i\frac{\omega}{\alpha^4}(\frac{2L}{c_0}-t)}\mathrm{d}\omega,$$

$$E_j(t,\alpha^2\boldsymbol{x},0^-) = \frac{\zeta_1^{\frac12}T_0}{(2\pi)^3}\iint \sum_{k=1}^2 \widehat{\mathcal{T}}^\alpha_{2j,2k}(\omega,\boldsymbol{\kappa},\boldsymbol{\kappa}',L)\widehat{b}^\alpha_{\mathrm{inc},k}(\omega,\boldsymbol{\kappa}') e^{i\boldsymbol{\kappa}\cdot\boldsymbol{x}}\mathrm{d}\boldsymbol{\kappa}'\mathrm{d}\boldsymbol{\kappa} e^{i\frac{\omega}{\alpha^4}(\frac{L}{c_1}-t)}\mathrm{d}\omega.$$

We first note that the rapid phase in ω is responsible for the localization in time of the transmitted and reflected waves (provided we show that $\widehat{\boldsymbol{\mathcal{T}}}^\alpha$ and $\widehat{\boldsymbol{\mathcal{R}}}^\alpha$ have limits) around times L/c_0 and $2L/c_0$, respectively. Therefore we focus our attention on the transmitted and reflected fields

$$\boldsymbol{E}^{\alpha,t}(s,\boldsymbol{x}) = \boldsymbol{E}\Big(t=\frac{L}{c_0}+\alpha^4 s,\alpha^2\boldsymbol{x},0^-\Big),$$
$$\boldsymbol{E}^{\alpha,r}(s,\boldsymbol{x}) = \boldsymbol{E}\Big(t=\frac{2L}{c_0}+\alpha^4 s,\alpha^2\boldsymbol{x},L^+\Big).$$

The proof of the convergence follows the strategy adopted in [24] to derive the paraxial wave equation from the acoustic wave equations. The proof is similar because the random components of the operator $\widehat{\boldsymbol{\mathcal{A}}}^\alpha$ have a diagonal block structure (with 2×2 blocks along the diagonal), which means that it has the same structure as the 2×2 operator encountered in the acoustic case. The main step of the proof consists in showing the convergence of the general moments of the transmitted and reflected wave components to the ones given by the limit system of stochastic partial differential equation (4.2). For $N\in\mathbb{N}$, $j_p,\tilde{j}_p\in\{1,2\}$, $m_p,\tilde{m}_p\in\mathbb{N}$, $s_p,\tilde{s}_p\in\mathbb{R}$ and $\boldsymbol{x}_p,\tilde{\boldsymbol{x}}_p\in\mathbb{R}^2$, $p=1,\dots,N$, the general moment of transmitted and reflected wave components

$$I^\alpha = \mathbb{E}\Big[\prod_{p=1}^N E^{\alpha,t}_{j_p}(s_p,\boldsymbol{x}_p)^{m_p}\prod_{p=1}^N E^{\alpha,r}_{\tilde{j}_p}(\tilde{s}_p,\tilde{\boldsymbol{x}}_p)^{\tilde{m}_p}\Big]$$

can be expressed as a sum of $2^{M+\tilde{M}}$ multiple integrals, for $M = \sum_{p=1}^{N} m_p$ and $\tilde{M} = \sum_{p=1}^{N} \tilde{m}_p$:

$$I^{\alpha} = \sum_{\substack{\boldsymbol{k}=(k_{p,h})_{h=1,\ldots,m_p,p=1,\ldots,N} \in \{1,2\}^{M} \\ \tilde{\boldsymbol{k}}=(\tilde{k}_{p,h})_{h=1,\ldots,\tilde{m}_p,p=1,\ldots,N} \in \{1,2\}^{\tilde{M}}}} I^{\alpha}_{\boldsymbol{k},\tilde{\boldsymbol{k}}}, \tag{5.17}$$

with

$$\begin{aligned} I^{\alpha}_{\boldsymbol{k},\tilde{\boldsymbol{k}}} = {} & \frac{\zeta_0^{\frac{M}{2}} \zeta_1^{\frac{\tilde{M}}{2}} T_0^{\tilde{M}}}{(2\pi)^{3(M+\tilde{M})}} \int \cdots \int \prod_{p=1}^{N} \prod_{h=1}^{m_p} \mathrm{d}\boldsymbol{\kappa}'_{p,h} \mathrm{d}\boldsymbol{\kappa}_{p,h} \mathrm{d}\omega_{p,h} \prod_{p=1}^{N} \prod_{h=1}^{\tilde{m}_p} \mathrm{d}\tilde{\boldsymbol{\kappa}}'_{p,h} \mathrm{d}\tilde{\boldsymbol{\kappa}}_{p,h} \mathrm{d}\tilde{\omega}_{p,h} \\ & \times \mathbb{E}\Big[\prod_{p=1}^{N} \prod_{h=1}^{m_p} \widehat{\mathcal{T}}^{\alpha}_{2j_p,2k_{p,h}}(\omega_{p,h}, \boldsymbol{\kappa}_{p,h}, \boldsymbol{\kappa}'_{p,h}, L) \prod_{p=1}^{N} \prod_{h=1}^{\tilde{m}_p} \widehat{\mathcal{R}}^{\alpha}_{2\tilde{j}_p-1,2\tilde{k}_{p,h}}(\tilde{\omega}_{p,h}, \tilde{\boldsymbol{\kappa}}_{p,h}, \tilde{\boldsymbol{\kappa}}'_{p,h}, L) \Big] \\ & \times \prod_{p=1}^{N} \prod_{h=1}^{m_p} \widehat{b}^{\alpha}_{\mathrm{inc},k_{p,h}}(\omega_{p,h}, \boldsymbol{\kappa}'_{p,h}) e^{i(\boldsymbol{\kappa}_{p,h} \cdot \boldsymbol{x}_p - \omega_{p,h} s_p)} \\ & \times \prod_{p=1}^{N} \prod_{h=1}^{\tilde{m}_p} \widehat{b}^{\alpha}_{\mathrm{inc},\tilde{k}_{p,h}}(\tilde{\omega}_{p,h}, \tilde{\boldsymbol{\kappa}}'_{p,h}) e^{i(\tilde{\boldsymbol{\kappa}}_{p,h} \cdot \tilde{\boldsymbol{x}}_p - \tilde{\omega}_{p,h} \tilde{s}_p)}. \end{aligned} \tag{5.18}$$

Therefore, the convergence of the general moments of the transmitted and reflected wave components in the white-noise limit will follow from the convergence of the specific moments $\mathbb{E}[\tilde{I}^{\alpha}(L)]$ of the transmission and reflection matrix operators, where

$$\tilde{I}^{\alpha}(z) = \prod_{p=1}^{M} \widehat{\mathcal{T}}^{\alpha}_{j_p k_p}(\omega_p, \boldsymbol{\kappa}_p, \boldsymbol{\kappa}'_p, z) \prod_{p=1}^{\tilde{M}} \widehat{\mathcal{R}}^{\alpha}_{\tilde{j}_p \tilde{k}_p}(\tilde{\omega}_p, \tilde{\boldsymbol{\kappa}}_p, \tilde{\boldsymbol{\kappa}}'_p, z). \tag{5.19}$$

We call these moments "specific" because we restrict our attention to the case in which the frequencies ω_p and $\tilde{\omega}_p$ are distinct. It is important to note that the reflection and transmission operators $\widehat{\boldsymbol{\mathcal{T}}}^{\alpha}$ and $\widehat{\boldsymbol{\mathcal{R}}}^{\alpha}$ themselves do not converge to $\widehat{\boldsymbol{\mathcal{T}}}$ and $\widehat{\boldsymbol{\mathcal{R}}}$, but only certain moments converge (expectations of products of components with distinct frequencies), which are those needed to ensure the convergence of the transmitted and reflected fields in view of (5.18).

We use diffusion approximation theorems as in [24] to obtain the characterization of the limits of the moments $\tilde{I}^{\alpha}$ as $\alpha \to 0$:

$$\lim_{\alpha \to 0} \mathbb{E}\big[\tilde{I}^{\alpha}(L)\big] = \mathbb{E}\Big[\prod_{p=1}^{M} \widehat{\mathcal{T}}_{j_p k_p}(\omega_p, \boldsymbol{\kappa}_p, \boldsymbol{\kappa}'_p, L) \prod_{p=1}^{\tilde{M}} \widehat{\mathcal{R}}_{\tilde{j}_p \tilde{k}_p}(\tilde{\omega}_p, \tilde{\boldsymbol{\kappa}}_p, \tilde{\boldsymbol{\kappa}}'_p, L) \Big],$$

when the right-hand side expectation is taken with respect to the following Itô-Schrödinger model for the transmission and reflection operators:

$$\widehat{\boldsymbol{\mathcal{T}}}(\omega, \boldsymbol{\kappa}, \boldsymbol{\kappa}', z) = \begin{bmatrix} \delta(\boldsymbol{\kappa} - \boldsymbol{\kappa}') & \widetilde{\mathcal{T}} & 0 & 0 \\ 0 & \widehat{\mathcal{T}} & 0 & 0 \\ 0 & 0 & \delta(\boldsymbol{\kappa} - \boldsymbol{\kappa}') & \widetilde{\mathcal{T}} \\ 0 & 0 & 0 & \widehat{\mathcal{T}} \end{bmatrix},$$

$$\widehat{\boldsymbol{\mathcal{R}}}(\omega, \boldsymbol{\kappa}, \boldsymbol{\kappa}', z) = \begin{bmatrix} \widetilde{\mathcal{R}} & \widehat{\mathcal{R}} & 0 & 0 \\ 0 & \delta(\boldsymbol{\kappa} - \boldsymbol{\kappa}') & 0 & 0 \\ 0 & 0 & \widetilde{\mathcal{R}} & \widehat{\mathcal{R}} \\ 0 & 0 & 0 & \delta(\boldsymbol{\kappa} - \boldsymbol{\kappa}') \end{bmatrix}.$$

The kernels $\widehat{\mathcal{T}}(\omega,\boldsymbol{\kappa},\boldsymbol{\kappa}',z)$, $\widehat{\mathcal{R}}(\omega,\boldsymbol{\kappa},\boldsymbol{\kappa}',z)$, and $\widetilde{\mathcal{R}}(\omega,\boldsymbol{\kappa},\boldsymbol{\kappa}',z)$ are solution of

$$\mathrm{d}\widehat{\mathcal{T}}(\omega,\boldsymbol{\kappa},\boldsymbol{\kappa}',z) = -\frac{ic_0|\boldsymbol{\kappa}'|^2}{2\omega}\widehat{\mathcal{T}}(\omega,\boldsymbol{\kappa},\boldsymbol{\kappa}',z)\mathrm{d}z - \frac{\omega^2 C_0(\mathbf{0})}{8c_0^2}\widehat{\mathcal{T}}(\omega,\boldsymbol{\kappa},\boldsymbol{\kappa}',z)\mathrm{d}z + \frac{i\omega}{2(2\pi)^2 c_0}\int \widehat{\mathcal{T}}(\omega,\boldsymbol{\kappa},\boldsymbol{\kappa}'',z)\mathrm{d}\widehat{B}(\boldsymbol{\kappa}''-\boldsymbol{\kappa}',z)\mathrm{d}\boldsymbol{\kappa}'',$$

starting from $\widehat{\mathcal{T}}(\omega,\boldsymbol{\kappa},\boldsymbol{\kappa}',z=0)=\delta(\boldsymbol{\kappa}-\boldsymbol{\kappa}')$,

$$\begin{aligned}\mathrm{d}\widehat{\mathcal{R}}(\omega,\boldsymbol{\kappa},\boldsymbol{\kappa}',z) &= -\frac{ic_0(|\boldsymbol{\kappa}|^2+|\boldsymbol{\kappa}'|^2)}{2\omega}\widehat{\mathcal{R}}(\omega,\boldsymbol{\kappa},\boldsymbol{\kappa}',z)\mathrm{d}z - \frac{\omega^2 C_0(\mathbf{0})}{4c_0^2}\widehat{\mathcal{R}}(\omega,\boldsymbol{\kappa},\boldsymbol{\kappa}',z)\mathrm{d}z\\ &-\frac{\omega^2}{4(2\pi)^2 c_0^2}\int \widehat{C}_0(\boldsymbol{\kappa}'')\widehat{\mathcal{R}}(\omega,\boldsymbol{\kappa}-\boldsymbol{\kappa}'',\boldsymbol{\kappa}'-\boldsymbol{\kappa}'',z)\mathrm{d}\boldsymbol{\kappa}''\mathrm{d}z\\ &+\frac{i\omega}{2(2\pi)^2 c_0}\int \Big(\widehat{\mathcal{R}}(\omega,\boldsymbol{\kappa},\boldsymbol{\kappa}'',z)\mathrm{d}\widehat{B}(\boldsymbol{\kappa}''-\boldsymbol{\kappa}',z)+\widehat{\mathcal{R}}(\omega,\boldsymbol{\kappa}'',\boldsymbol{\kappa}',z)\mathrm{d}\widehat{B}(\boldsymbol{\kappa}-\boldsymbol{\kappa}'',z)\Big)\mathrm{d}\boldsymbol{\kappa}'',\end{aligned}$$

starting from $\widehat{\mathcal{R}}(\omega,\boldsymbol{\kappa},\boldsymbol{\kappa}',z=0)=R_0\delta(\boldsymbol{\kappa}-\boldsymbol{\kappa}')$, and

$$\mathrm{d}\widetilde{\mathcal{R}}(\omega,\boldsymbol{\kappa},\boldsymbol{\kappa}',z) = -\frac{ic_0|\boldsymbol{\kappa}|^2}{2\omega}\widetilde{\mathcal{R}}(\omega,\boldsymbol{\kappa},\boldsymbol{\kappa}',z)\mathrm{d}z - \frac{\omega^2 C_0(\mathbf{0})}{8c_0^2}\widetilde{\mathcal{R}}(\omega,\boldsymbol{\kappa},\boldsymbol{\kappa}',z)\mathrm{d}z + \frac{i\omega}{2(2\pi)^2 c_0}\int \widetilde{\mathcal{R}}(\omega,\boldsymbol{\kappa}'',\boldsymbol{\kappa}',z)\mathrm{d}\widehat{B}(\boldsymbol{\kappa}-\boldsymbol{\kappa}'',z)\mathrm{d}\boldsymbol{\kappa}'',$$

starting from $\widetilde{\mathcal{R}}(\omega,\boldsymbol{\kappa},\boldsymbol{\kappa}',z=0)=\delta(\boldsymbol{\kappa}-\boldsymbol{\kappa}')$. Finally $\widetilde{\mathcal{T}}(\omega,\boldsymbol{\kappa},\boldsymbol{\kappa}',z)=R_0\widehat{\mathcal{T}}(\omega,\boldsymbol{\kappa},\boldsymbol{\kappa}',z)$. Here the Brownian field $\widehat{B}$ is the partial Fourier transform of the Brownian field B with covariance (4.4). It has the following operator-valued spatial covariance

$$\mathbb{E}\big[\widehat{B}(\boldsymbol{\kappa},z)\widehat{B}(\boldsymbol{\kappa}',z')\big] = \min\{z,z'\}(2\pi)^2\widehat{C}_0(\boldsymbol{\kappa})\delta(\boldsymbol{\kappa}+\boldsymbol{\kappa}').$$

By considering the transmission and reflection matrix operator in the original spatial variables,

$$\begin{aligned}\breve{\mathcal{T}}(\omega,\boldsymbol{x},\boldsymbol{x}',z) &= \frac{T_0}{(2\pi)^2}\iint e^{i(\boldsymbol{\kappa}\cdot\boldsymbol{x}-\boldsymbol{\kappa}'\cdot\boldsymbol{x}')}\widehat{\mathcal{T}}(\omega,\boldsymbol{\kappa},\boldsymbol{\kappa}',z)\mathrm{d}\boldsymbol{\kappa}\mathrm{d}\boldsymbol{\kappa}',\\ \breve{\mathcal{R}}(\omega,\boldsymbol{x},\boldsymbol{x}',z) &= \frac{1}{(2\pi)^2}\iint e^{i(\boldsymbol{\kappa}\cdot\boldsymbol{x}-\boldsymbol{\kappa}'\cdot\boldsymbol{x}')}\widehat{\mathcal{R}}(\omega,\boldsymbol{\kappa},\boldsymbol{\kappa}',z)\mathrm{d}\boldsymbol{\kappa}\mathrm{d}\boldsymbol{\kappa}',\end{aligned}$$

we obtain that they satisfy the systems (4.2) and (4.7) where we use the Stratonovich integral instead of Itô.

6. The Wigner distributions of the transmitted and reflected fields. As mentioned in the introduction, the Itô-Schrödinger model is very convenient in order to compute the statistical properties of the transmitted and reflected waves, since the moment equations are closed at any order. The analysis of the second-order moments allows us to get the autocorrelation functions of the waves, or equivalently the Wigner distributions which are determined by a closed system of transport equations [14, 15, 24, 29].

Let us denote by ω_0 the carrier frequency and by B the bandwidth of the source. We consider two frequencies ω_1 and ω_2 in the spectrum centered at ω_0 and we define

the two-frequency Wigner distribution of the transmission operator by

$$W^T(\boldsymbol{x},\boldsymbol{x}',\boldsymbol{\kappa},\boldsymbol{\kappa}',z)=\frac{1}{(2\pi)^2}\iint \mathrm{d}\boldsymbol{y}\mathrm{d}\boldsymbol{y}' e^{-i(\boldsymbol{\kappa}\cdot\boldsymbol{y}-\boldsymbol{\kappa}'\cdot\boldsymbol{y}')} \tag{6.1}$$
$$\times\mathbb{E}\Big[\check{T}\Big(\omega_1,\frac{\sqrt{\omega_0}}{\sqrt{\omega_1}}(\boldsymbol{x}+\frac{\boldsymbol{y}}{2}),\frac{\sqrt{\omega_0}}{\sqrt{\omega_1}}(\boldsymbol{x}'+\frac{\boldsymbol{y}'}{2}),z\Big)\overline{\check{T}}\Big(\omega_2,\frac{\sqrt{\omega_0}}{\sqrt{\omega_2}}(\boldsymbol{x}-\frac{\boldsymbol{y}}{2}),\frac{\sqrt{\omega_0}}{\sqrt{\omega_2}}(\boldsymbol{x}'-\frac{\boldsymbol{y}'}{2}),z\Big)\Big].$$

Using the Itô-Schrödinger equation (4.2) and Itô's formula, we find that the Wigner distribution satisfies the closed system

$$\frac{\partial W^T}{\partial z}-\frac{c_0\boldsymbol{\kappa}'}{\omega_0}\cdot\nabla_{\boldsymbol{x}'}W^T=-\frac{C_0(\mathbf{0})(\omega_1^2+\omega_2^2)}{8c_0^2}W^T(\boldsymbol{x},\boldsymbol{x}',\boldsymbol{\kappa},\boldsymbol{\kappa}',z)$$
$$+\frac{\omega_1\omega_2}{4(2\pi)^2c_0^2}\int\widehat{C}_0(\boldsymbol{u})e^{i\boldsymbol{u}\cdot\boldsymbol{x}'\left(\frac{\sqrt{\omega_0}}{\sqrt{\omega_1}}-\frac{\sqrt{\omega_0}}{\sqrt{\omega_2}}\right)}W^T\Big(\boldsymbol{x},\boldsymbol{x}',\boldsymbol{\kappa},\boldsymbol{\kappa}'+\frac{1}{2}(\frac{\sqrt{\omega_0}}{\sqrt{\omega_1}}+\frac{\sqrt{\omega_0}}{\sqrt{\omega_2}})\boldsymbol{u},z\Big)\mathrm{d}\boldsymbol{u},$$

starting from

$$W^T(\boldsymbol{x},\boldsymbol{x}',\boldsymbol{\kappa},\boldsymbol{\kappa}',z=0)=T_0^2\frac{\omega_1\omega_2}{\omega_0^2}\delta(\boldsymbol{x}-\boldsymbol{x}')\delta(\boldsymbol{\kappa}-\boldsymbol{\kappa}').$$

It is possible to solve this system and to find an integral representation of the two-frequency Wigner distribution by using the approach of [14]. However, this representation can be simplified if the bandwidth B of the source is much smaller than the carrier frequency ω_0. In this regime, if ω_1,ω_2 lie in the spectrum of the source, then the two-frequency Wigner distribution W^T depends only on the carrier frequency ω_0 and not on the lag $\omega_1-\omega_2$. The Wigner distribution satisfies

$$\frac{\partial W^T}{\partial z}-\frac{c_0\boldsymbol{\kappa}'}{\omega_0}\cdot\nabla_{\boldsymbol{x}'}W^T=\frac{\omega_0^2}{4(2\pi)^2c_0^2}\int\widehat{C}_0(\boldsymbol{u})\Big[W^T\big(\boldsymbol{x},\boldsymbol{x}',\boldsymbol{\kappa},\boldsymbol{\kappa}'+\boldsymbol{u},z\big)$$
$$-W^T\big(\boldsymbol{x},\boldsymbol{x}',\boldsymbol{\kappa},\boldsymbol{\kappa}',z\big)\Big]\mathrm{d}\boldsymbol{u}, \tag{6.2}$$

starting from $W^T(\boldsymbol{x},\boldsymbol{x}',\boldsymbol{\kappa},\boldsymbol{\kappa}',z=0)=T_0^2\delta(\boldsymbol{x}-\boldsymbol{x}')\delta(\boldsymbol{\kappa}-\boldsymbol{\kappa}')$. We remark that the equation for W^T has a form similar to the radiative transport equation for angularly-resolved wave energy density. However, the equation for W^T has been established by taking into account all incoherent and coherent effects. By taking a Fourier transform in $\boldsymbol{\kappa}'$ and $\boldsymbol{x}'$ of (6.2), we obtain an equation that can be integrated and we find the following integral representation for W^T:

$$W^T(\boldsymbol{x},\boldsymbol{x}',\boldsymbol{\kappa},\boldsymbol{\kappa}',z)=\frac{{T_0}^2}{(2\pi)^4}\iint e^{i(\boldsymbol{\kappa}'-\boldsymbol{\kappa})\cdot\boldsymbol{y}_1}e^{-i\left(\boldsymbol{x}'-\boldsymbol{x}+\frac{c_0\boldsymbol{\kappa}}{\omega_0}z\right)\cdot\boldsymbol{\kappa}_1}$$
$$\times e^{\frac{\omega_0^2}{4c_0^2}\int_0^z C_0(\boldsymbol{y}_1+\frac{c_0\boldsymbol{\kappa}_1}{\omega_0}z')-C_0(\mathbf{0})\mathrm{d}z'}\mathrm{d}\boldsymbol{y}_1\mathrm{d}\boldsymbol{\kappa}_1. \tag{6.3}$$

The function W^T can be interpreted as the kernel of the operator that gives the Wigner distribution W^E of the transmitted field in terms of the Wigner distribution W^J of the source. Indeed the Wigner distribution of the transmitted field:

$$W^E_{j,l}(s_1,s_2,\boldsymbol{x},\boldsymbol{\kappa})=\int\mathbb{E}\Big[E_j^{(t)}\big(s_1,\boldsymbol{x}+\frac{\boldsymbol{y}}{2}\big)E_l^{(t)}\big(s_2,\boldsymbol{x}-\frac{\boldsymbol{y}}{2}\big)\Big]e^{-i\boldsymbol{\kappa}\cdot\boldsymbol{y}}\mathrm{d}\boldsymbol{y}$$

can be obtained through the formula (for $j,l=1,2$)

$$W^E_{j,l}(s_1,s_2,\boldsymbol{x},\boldsymbol{\kappa})=\frac{\zeta_0\zeta_1}{4}\iint W^T(\boldsymbol{x},\boldsymbol{x}',\boldsymbol{\kappa},\boldsymbol{\kappa}',L)W^J_{j,l}(s_1,s_2,\boldsymbol{x}',\boldsymbol{\kappa}')\mathrm{d}\boldsymbol{x}'\mathrm{d}\boldsymbol{\kappa}', \tag{6.4}$$
$$W^J_{j,l}(s_1,s_2,\boldsymbol{x}',\boldsymbol{\kappa}')=\int J_j\big(s_1,\boldsymbol{x}'+\frac{\boldsymbol{y}'}{2}\big)J_l\big(s_2,\boldsymbol{x}'-\frac{\boldsymbol{y}'}{2}\big)e^{-i\boldsymbol{\kappa}'\cdot\boldsymbol{y}'}\mathrm{d}\boldsymbol{y}'.$$

We now define the two-frequency Wigner distribution of the reflection operator by

$$W^R(\boldsymbol{x},\boldsymbol{x}',\boldsymbol{\kappa},\boldsymbol{\kappa}',z)=\frac{1}{(2\pi)^2}\iint \mathrm{d}\boldsymbol{y}\mathrm{d}\boldsymbol{y}' e^{-i(\boldsymbol{\kappa}\cdot\boldsymbol{y}-\boldsymbol{\kappa}'\cdot\boldsymbol{y}')} \tag{6.5}$$
$$\times\mathbb{E}\Big[\breve{\mathcal{R}}\big(\omega_1,\frac{\sqrt{\omega_0}}{\sqrt{\omega_1}}(\boldsymbol{x}+\frac{\boldsymbol{y}}{2}),\frac{\sqrt{\omega_0}}{\sqrt{\omega_1}}(\boldsymbol{x}'+\frac{\boldsymbol{y}'}{2}),z\big)\overline{\breve{\mathcal{R}}}\big(\omega_2,\frac{\sqrt{\omega_0}}{\sqrt{\omega_2}}(\boldsymbol{x}-\frac{\boldsymbol{y}}{2}),\frac{\sqrt{\omega_0}}{\sqrt{\omega_2}}(\boldsymbol{x}'-\frac{\boldsymbol{y}'}{2}),z\big)\Big].$$

If the bandwidth is small and if ω_1,ω_2 lie in the spectrum of the wave, then we find that the two-frequency Wigner distribution W^R depends only on the carrier frequency ω_0 and not on the lag $\omega_1-\omega_2$. The Wigner distribution then satisfies the closed system

$$\begin{aligned}&\frac{\partial W^R}{\partial z}+\frac{c_0}{\omega_0}(\boldsymbol{\kappa}\cdot\nabla_{\boldsymbol{x}}-\boldsymbol{\kappa}'\cdot\nabla_{\boldsymbol{x}'})W^R\\&=\frac{\omega_0^2}{4(2\pi)^2c_0^2}\int\widehat{C}_0(\boldsymbol{u})\Big[W^R(\boldsymbol{x},\boldsymbol{x}',\boldsymbol{\kappa}-\boldsymbol{u},\boldsymbol{\kappa}',z)+W^R(\boldsymbol{x},\boldsymbol{x}',\boldsymbol{\kappa},\boldsymbol{\kappa}'+\boldsymbol{u},z)\\&\qquad-2W^R(\boldsymbol{x},\boldsymbol{x}',\boldsymbol{\kappa},\boldsymbol{\kappa}',z)+2W^R(\boldsymbol{x},\boldsymbol{x}',\boldsymbol{\kappa}-\frac{1}{2}\boldsymbol{u},\boldsymbol{\kappa}'+\frac{1}{2}\boldsymbol{u},z)\cos\big(\boldsymbol{u}\cdot(\boldsymbol{x}-\boldsymbol{x}')\big)\\&\qquad-2W^R(\boldsymbol{x},\boldsymbol{x}',\boldsymbol{\kappa}-\frac{1}{2}\boldsymbol{u},\boldsymbol{\kappa}'-\frac{1}{2}\boldsymbol{u},z)\cos\big(\boldsymbol{u}\cdot(\boldsymbol{x}-\boldsymbol{x}')\big)\Big]\mathrm{d}\boldsymbol{u},\end{aligned} \tag{6.6}$$

starting from $W^R(\boldsymbol{x},\boldsymbol{x}',\boldsymbol{\kappa},\boldsymbol{\kappa}',z=0)=R_0^2\delta(\boldsymbol{x}-\boldsymbol{x}')\delta(\boldsymbol{\kappa}-\boldsymbol{\kappa}')$. The Wigner distribution of the reflected field is given in terms of the Wigner distribution of the source by (6.4) with W^R instead of W^T and with the multiplicative factor $\zeta_0^2/4$ instead of $\zeta_0\zeta_1/4$. The Wigner transform of the reflection operator contains all incoherent and coherent effects, and we will see in the next section that it accounts for instance for the enhanced backscattering phenomenon.

7. Electromagnetic coherence and applications.

7.1. Enhanced backscattering. In this section we illustrate the fact that the Itô-Schrödinger model captures all coherent effects. We here generalize the results obtained in [24] to show that the reflected power exhibits a singular picture in a very narrow cone around the backscattered direction. This phenomenon, observed in particular in the context of backscattering from a heterogeneous medium, is called enhanced backscattering or weak localization and is extensively discussed in the physical literature [5, 30]. The physical observation is that, for an incoming quasi-monochromatic quasi-plane wave, the mean reflected power has a local maximum in the backscattered direction, which is twice as large as the mean reflected power in the other directions (Figure 7.1). The physical explanation is that the enhanced backscattering phenomenon results from constructive interference between a multiply scattered ray and its time-reversed counterpart. It can also be observed in the context of scattering from rough surfaces [27]. Moreover, similar physics manifests in closed ballistic systems or strongly multiple scattering system [12, 35], where the enhancement can exceed a factor of two.

In this section the source has the form

$$\boldsymbol{J}(t,\boldsymbol{x})=f(t)e^{-i\omega_0 t}\boldsymbol{g}(\boldsymbol{x})+c.c.,$$

where *c.c.* means complex conjugate. We assume that it is narrowband around the carrier frequency ω_0, and that it generates a quasi-plane wave, in the sense that $\hat{\boldsymbol{g}}(\boldsymbol{\kappa})$ is concentrated at some $\boldsymbol{\kappa}_{\mathrm{inc}}$. By "concentrated" we mean that the diameter of the

support of $\hat{\boldsymbol{g}}(\boldsymbol{\kappa})$ is smaller than $k_0^2 l_x^2/L$, where l_x is the transverse correlation radius of the random fluctuations of the medium and $k_0 = \omega_0/c_0$ is the carrier wavenumber.

In the asymptotic regime $\alpha \to 0$, the reflected wave in the $\boldsymbol{\kappa}$-direction is

$$\hat{\boldsymbol{E}}^{(r)}(s,\boldsymbol{\kappa}) = \int \boldsymbol{E}^{(r)}(s,\boldsymbol{x}) e^{-i\boldsymbol{\kappa}\cdot\boldsymbol{x}} \mathrm{d}\boldsymbol{x},$$

where $\boldsymbol{E}^{(r)}$ is the solution of the Itô-Schrödinger model of Proposition 4.2. In the Fraunhofer regime $k_0 l_x^2 \ll L$, using the same method as in [24], we find from (6.6) that the mean reflected intensity of the j-th polarization in the $\boldsymbol{\kappa}$-direction is of the form:

$$\mathbb{E}\big[|\hat{E}_j^{(r)}(s,\boldsymbol{\kappa})|^2\big] = \frac{\zeta_0^2}{4} R_0^2 |f(s)|^2 P_j I^{(r)}(\boldsymbol{\kappa}), \quad j = 1,2, \tag{7.1}$$

$$I^{(r)}(\boldsymbol{\kappa}) = \mathcal{V}_{\boldsymbol{0}}^{(r)}(\boldsymbol{\kappa} - \boldsymbol{\kappa}_{\mathrm{inc}}) + \mathcal{V}_{\boldsymbol{\kappa}+\boldsymbol{\kappa}_{\mathrm{inc}}}^{(r)}(\boldsymbol{\kappa} - \boldsymbol{\kappa}_{\mathrm{inc}}) - e^{-\frac{k_0^2}{2} C_0(\boldsymbol{0}) L} \delta(\boldsymbol{\kappa} - \boldsymbol{\kappa}_{\mathrm{inc}}), \tag{7.2}$$

where $P_j = \int |\hat{g}_j(\boldsymbol{\kappa})|^2 \mathrm{d}\boldsymbol{\kappa}$ and

$$\mathcal{V}_{\boldsymbol{\kappa}'}^{(r)}(\boldsymbol{\kappa}) = \frac{1}{4\pi^2} \int e^{-i\boldsymbol{\kappa}\cdot\boldsymbol{u}} e^{\frac{k_0^2}{4} \int_{-L}^{L} C_0(\boldsymbol{u} + \frac{z}{k_0}\boldsymbol{\kappa}') - C_0(\boldsymbol{0}) \mathrm{d}z} \mathrm{d}\boldsymbol{u}. \tag{7.3}$$

In absence of random scattering $C_0 \equiv 0$, we have the usual specular reflection

$$I^{(r)}(\boldsymbol{\kappa})\big|_{C_0 \equiv 0} = \delta(\boldsymbol{\kappa} - \boldsymbol{\kappa}_{\mathrm{inc}}).$$

In the presence of random scattering, the specular reflection takes the form of a Dirac peak at $\boldsymbol{\kappa}_{\mathrm{inc}}$ with intensity $\exp(-k_0^2 C_0(\boldsymbol{0}) L/2)$ and a diffusive cone centered at $\boldsymbol{\kappa}_{\mathrm{inc}}$. More exactly, far enough from the backscattered direction $-\boldsymbol{\kappa}_{\mathrm{inc}}$, the reflected intensity is

$$\begin{aligned} I^{(r)}(\boldsymbol{\kappa}) &= \mathcal{V}_{\boldsymbol{0}}^{(r)}(\boldsymbol{\kappa} - \boldsymbol{\kappa}_{\mathrm{inc}}) \quad \text{for } |\boldsymbol{\kappa} + \boldsymbol{\kappa}_{\mathrm{inc}}| L \gg k_0 l_x \\ &= e^{-\frac{k_0^2}{2} C_0(\boldsymbol{0}) L} \Big[\delta(\boldsymbol{\kappa} - \boldsymbol{\kappa}_{\mathrm{inc}}) + \frac{1}{4\pi^2} \int e^{-i(\boldsymbol{\kappa} - \boldsymbol{\kappa}_{\mathrm{inc}})\cdot\boldsymbol{u}} \big(e^{\frac{k_0^2}{2} C_0(\boldsymbol{u}) L} - 1 \big) \mathrm{d}\boldsymbol{u} \Big]. \end{aligned} \tag{7.4}$$

In a narrow cone around the backscattered direction $-\boldsymbol{\kappa}_{\mathrm{inc}}$, the reflected intensity is locally larger and given by (7.2). The maximal enhancement factor (compared to (7.4)) is reached at the backscattered direction $-\boldsymbol{\kappa}_{\mathrm{inc}}$ and it is equal to 2. It is possible to give explicit expressions for the shape of the enhanced backscattering cone in the strong scattering regime, as we show below.

Let us assume that $k_0^2 C_0(\boldsymbol{0}) L \gg 1$ (which means that random scattering is strong and that the coherent specular peak is vanishing) and that the correlation function C_0 is twice differentiable at zero: $C_0(\boldsymbol{x}) = C_0(\boldsymbol{0}) - \frac{D_0}{2}|\boldsymbol{x}|^2 + o(|\boldsymbol{x}|^2)$ (which means that the fluctuations of the medium are smooth and isotropic),

$$D_0 = -\frac{1}{2} \Delta C_0(\boldsymbol{0}) = \frac{1}{8\pi^2} \int |\boldsymbol{\kappa}|^2 \widehat{C}_0(\boldsymbol{\kappa}) \mathrm{d}\boldsymbol{\kappa}.$$

Physically, if we denote by σ (resp. l_x, l_z) the standard deviation (resp. the transverse correlation radius, the longitudinal correlation radius) of $n_\varepsilon + n_\mu$, then $C_0(\boldsymbol{0}) \sim \sigma^2 l_z$ and $D_0 \sim \sigma^2 l_z l_x^{-2}$.

The expression (7.4) of the specular cone can then be simplified to:

$$I^{(r)}(\boldsymbol{\kappa}) = \frac{1}{\pi k_0^2 D_0 L} e^{-\frac{1}{k_0^2 D_0 L} |\boldsymbol{\kappa} - \boldsymbol{\kappa}_{\mathrm{inc}}|^2} \quad \text{for } |\boldsymbol{\kappa} + \boldsymbol{\kappa}_{\mathrm{inc}}| L \gg k_0 l_x. \tag{7.5}$$

This formula gives the width of the diffusive cone around the specular direction $\boldsymbol{\kappa}_{\rm inc}$:

$$\Delta\kappa_{\rm spec} = \sqrt{D_0 L} k_0, \qquad \Delta\theta_{\rm spec} = \sqrt{D_0 L}, \tag{7.6}$$

where the angular width is defined by $\Delta\theta_{\rm spec} = \Delta\kappa_{\rm spec}/k_0$. On the top of this broad cone, we have a narrow cone of relative maximum equal to 2 centered along the backscattered direction $-\boldsymbol{\kappa}_{\rm inc}$:

$$I^{(r)}(\boldsymbol{\kappa}) = \frac{1}{\pi k_0^2 D_0 L} e^{-\frac{1}{k_0^2 D_0 L}|\boldsymbol{\kappa}-\boldsymbol{\kappa}_{\rm inc}|^2} \Big[1 + e^{-\frac{D_0 L^3}{12}|\boldsymbol{\kappa}+\boldsymbol{\kappa}_{\rm inc}|^2}\Big]. \tag{7.7}$$

This shows that the width of the enhanced backscattering cone is

$$\Delta\kappa_{\rm EBC} = \frac{\sqrt{12}}{\sqrt{D_0 L^3}}, \qquad \Delta\theta_{\rm EBC} = \frac{\sqrt{12}}{k_0\sqrt{D_0 L^3}}. \tag{7.8}$$

Note that the angular width $\Delta\theta_{\rm EBC}$ of the cone is proportional to the wavelength, as predicted by physical arguments based on diagrammatic expansions [30]. As discussed in Subsection 7.3 these formulas can be used in tomography for the measurements of the scattering coefficient and the interface location.

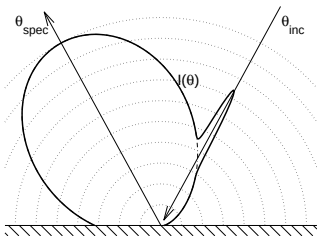

FIG. 7.1. *Schematic for the enhanced backscattering phenomenon: when an incoming quasi-plane wave traveling through a random medium is reflected by an interface, the mean angularly-resolved reflected power (solid line) consists of a broad diffusive cone around the specular direction and on the top of it a narrow cone of relative maximum equal to two centered around the backscattered direction.*

7.2. Time reversal. We here discuss application to time reversal. A time reversal mirror (TRM) is an array of antennas that can be used either as receivers or as emitters. Consider the case in which a source emits a signal that is captured on a TRM, then stored and resent in the reverse direction of time, that is "last in first out". Depending on the size of the TRM the signal will then refocus tightly at the original source location. This general problem has received much attention from both the experimental and mathematical viewpoints and has a number of applications [17, 19]. In a random medium the angular spread of the forward propagating wave can be much wider than in a homogeneous medium, while the correlation radius can be much smaller. This duality can in fact create a better refocusing in the random medium as compared to the homogeneous medium as the refocusing is a coherence phenomenon [15].

In the first part of the time reversal experiment the electromagnetic source is located at $z = L$ as in (2.9). The TRM is located at $z = 0$ and is used as an array of receivers. Its transverse spatial support has a radius of order α^2 and is denoted

by $\alpha^2 D \subset \mathbb{R}^2$. It records the field during the time interval $[L/c_0 - \alpha^4 T, L/c_0 + \alpha^4 T]$, with center at the expected travel time L/c_0 and with width $2\alpha^4 T$. The TRM records part or all of the components of the electromagnetic field. The recorded field is

$$\begin{bmatrix} \boldsymbol{E}^{(\mathrm{rec})} \\ \boldsymbol{H}^{(\mathrm{rec})} \end{bmatrix}(s, \boldsymbol{x}) = \begin{bmatrix} \mathbf{A}^{(E)} & \mathbf{0} \\ \mathbf{0} & \mathbf{A}^{(H)} \end{bmatrix} \begin{bmatrix} \boldsymbol{E} \\ \boldsymbol{H} \end{bmatrix} \Big(\frac{L}{c_0} + \alpha^4 s, \alpha^2 \boldsymbol{x}, z = 0 \Big), \quad s \in [-T, T], \quad \boldsymbol{x} \in D,$$

where $\mathbf{A}^{(E)}$ and $\mathbf{A}^{(H)}$ are 3×3 diagonal matrices whose nonzero elements correspond to the components of the electromagnetic field that are recorded by the TRM.

In the second part of the time reversal experiment the recorded signal is time-reversed in memory, and sent back in the medium by the TRM used as an array of emitters. The new source is

$$\begin{aligned} \boldsymbol{J}^{(s)}_{\mathrm{mir}}(t, \boldsymbol{x}, z) &= \boldsymbol{J}_{\mathrm{mir}}\Big(\frac{t}{\alpha^4}, \frac{\boldsymbol{x}}{\alpha^2} \Big)\ \delta(z), \\ \boldsymbol{J}_{\mathrm{mir}}(s, \boldsymbol{x}) &= \big[\zeta_0^{-1} \mathbf{B}^{(E)} \boldsymbol{E}^{(\mathrm{rec})}(-s, \boldsymbol{x}) + \mathbf{B}^{(H)} \boldsymbol{H}^{(\mathrm{rec})}(-s, \boldsymbol{x}) \big] \chi_{\mathrm{t}}\Big(\frac{s}{T} \Big) \chi_{\mathrm{x}}\Big(\frac{\boldsymbol{x}}{A} \Big), \end{aligned}$$

where $\mathbf{B}^{(E)}$ and $\mathbf{B}^{(H)}$ are 3×3 constant coupling matrices that scramble the measurements, $2\alpha^4 T$ is the recording time duration, and $\alpha^2 A$ is the radius of the TRM. The functions χ_{x} and χ_{t} are normalized space and time windows for the resent signal, they can be either characteristic functions of the time-space domain where the electromagnetic field is recorded or some other functions that allow for space-time dependent amplification of the resent signal. In the small-α limit the refocused field observed in the original source plane $z = L$:

$$\begin{bmatrix} \boldsymbol{E}^{(\mathrm{ref})} \\ \boldsymbol{H}^{(\mathrm{ref})} \end{bmatrix}(s, \boldsymbol{x}) = \begin{bmatrix} \boldsymbol{E} \\ \boldsymbol{H} \end{bmatrix} \Big(\frac{L}{c_0} + \alpha^4 s, \alpha^2 \boldsymbol{x}, z = L \Big)$$

can be expressed as

$$E^{(\mathrm{ref})}_j(s, \boldsymbol{x}) = -\frac{\zeta_0}{4\pi} \iint \breve{\mathcal{T}}(\omega, \boldsymbol{x}, \boldsymbol{x}', L, 0) \breve{J}_{j,\mathrm{mir}}(\omega, \boldsymbol{x}') \mathrm{d}\boldsymbol{x}' e^{-i\omega s} \mathrm{d}\omega, \quad j = 1, 2,$$

$E^{(\mathrm{ref})}_3 = 0$, $H^{(\mathrm{ref})}_1 = \zeta_0^{-1} E^{(\mathrm{ref})}_2$, $H^{(\mathrm{ref})}_2 = -\zeta_0^{-1} E^{(\mathrm{ref})}_1$, and $H^{(\mathrm{ref})}_3 = 0$. Here we wrote $\breve{\mathcal{T}}(\omega, \boldsymbol{x}, \boldsymbol{x}', L, 0)$ for the time-harmonic transmission kernel corresponding to propagation from the plane $z = 0$ to the plane $z = L$.

The source terms of the TRM can be written in the form ($j = 1, 2$):

$$\begin{aligned} \breve{J}_{\mathrm{mir},j}(\omega, \boldsymbol{x}) &= -\frac{1}{4\pi} \int \overline{\breve{\mathcal{T}}}(\omega', \boldsymbol{x}, \boldsymbol{x}', 0, L) \breve{J}_{\mathrm{eff},j}(\omega', \boldsymbol{x}') \chi_{\mathrm{x}}\Big(\frac{\boldsymbol{x}}{A} \Big) \breve{\chi}_{\mathrm{t}}(T(\omega - \omega')) T\, \mathrm{d}\omega' \\ \breve{J}_{\mathrm{eff},j}(\omega, \boldsymbol{x}) &= \Big(B^{(1)}_{j1} A^{(1)}_{j1} - B^{(2)}_{j2} A^{(2)}_{j2} \Big) \overline{\breve{J}}_1(\omega, \boldsymbol{x}) + \Big(B^{(1)}_{j2} A^{(1)}_{j2} + B^{(2)}_{j2} A^{(2)}_{j2} \Big) \overline{\breve{J}}_2(\omega, \boldsymbol{x}). \end{aligned}$$

The refocused field can then be written as ($j = 1, 2$):

$$E^{(\mathrm{ref})}_j\big(s, \boldsymbol{x}\big) = \frac{\zeta_0}{4} \iint \breve{\mathcal{K}}(\omega, \boldsymbol{x}, \boldsymbol{x}') \breve{J}_{\mathrm{eff},j}(\omega, \boldsymbol{x}') \mathrm{d}\boldsymbol{x}' e^{-i\omega s} \mathrm{d}\omega,$$

with the refocusing kernel being

$$\begin{aligned} \breve{\mathcal{K}}(\omega, \boldsymbol{x}, \boldsymbol{x}') = \frac{1}{(2\pi)^2} \iint & \breve{\mathcal{T}}(\omega, \boldsymbol{x}, \boldsymbol{x}'', L, 0) \overline{\breve{\mathcal{T}}}(\omega', \boldsymbol{x}', \boldsymbol{x}'', L, 0) \\ & \times \chi_{\mathrm{x}}\Big(\frac{\boldsymbol{x}''}{A} \Big) \breve{\chi}_{\mathrm{t}}\big(T(\omega - \omega')\big) T\, \mathrm{d}\omega' \mathrm{d}\boldsymbol{x}'', \end{aligned} \tag{7.9}$$

where we have used the reciprocity identity $\breve{\mathcal{T}}(\omega', \boldsymbol{x}'', \boldsymbol{x}', 0, L) = \breve{\mathcal{T}}(\omega', \boldsymbol{x}', \boldsymbol{x}'', L, 0)$. We can use the two frequency Wigner distribution to obtain an expression for the mean refocusing kernel. We again obtain a simplified expression in the regime when the carrier frequency ω_0 of the source is larger than its bandwidth B and when the recording time T is larger than the duration of the source $1/B$. In this regime we find that the expression for the mean refocusing kernel for ω is the bandwidth of the source is

$$\begin{aligned}\mathbb{E}\big[\breve{\mathcal{K}}(\omega, \boldsymbol{x}, \boldsymbol{x}')\big] &= \frac{\chi_{\mathrm{t}}(0)}{(2\pi)^3} \iint W^T\Big(\frac{\boldsymbol{x}+\boldsymbol{x}'}{2}, \boldsymbol{x}'', \boldsymbol{\kappa}, \boldsymbol{\kappa}', L\Big) e^{i\boldsymbol{\kappa}\cdot(\boldsymbol{x}-\boldsymbol{x}')} \chi_{\mathrm{x}}\Big(\frac{\boldsymbol{x}''}{A}\Big) \mathrm{d}\boldsymbol{\kappa} \mathrm{d}\boldsymbol{\kappa}' \mathrm{d}\boldsymbol{x}'' \\ &= \frac{A^2\omega_0^2\chi_{\mathrm{t}}(0)}{(2\pi)^3(c_0L)^2} e^{i\frac{\omega_0}{c_0}\frac{|\boldsymbol{x}|^2-|\boldsymbol{x}'|^2}{2L}} e^{\frac{\omega_0^2\ell_z L}{4c_0^2}\int_0^1 \tilde{C}_0(s|\boldsymbol{x}-\boldsymbol{x}'|/\ell_x)-\tilde{C}_0(0)\mathrm{d}s} \hat{\chi}_{\mathrm{x}}\Big(\frac{(\boldsymbol{x}-\boldsymbol{x}')\omega_0 A}{c_0 L}\Big),\end{aligned}$$

where we assumed that the covariance function has the form $C_0(\boldsymbol{x}) = l_z \tilde{C}_0\left(|\boldsymbol{x}|/\ell_x\right)$, for $\tilde{C}_0$ a normalized shape function, l_z the longitudinal correlation length, and l_x the transverse correlation length.

We now assume that the medium Fresnel length is large compared to the central wavelength: $\sqrt{\ell_z L} \gg \lambda_0$. Then we obtain the characterization

$$\mathbb{E}\big[\breve{\mathcal{K}}(\omega, \boldsymbol{x}, \boldsymbol{x}')\big] = \frac{A^2\omega_0^2\chi_{\mathrm{t}}(0)}{(2\pi)^3(c_0L)^2} e^{i\frac{\omega_0}{c_0}\frac{|\boldsymbol{x}|^2-|\boldsymbol{x}'|^2}{2L}} e^{\frac{\omega_0^2 L\ell_z \tilde{C}_0''(0)|\boldsymbol{x}-\boldsymbol{x}'|^2}{24\ell_x^2 c_0^2}} \hat{\chi}_{\mathrm{x}}\Big(\frac{(\boldsymbol{x}-\boldsymbol{x}')\omega_0 A}{c_0 L}\Big).$$

The spatial support of the refocusing kernel in the case without random medium effects is the classic Rayleigh resolution $\mathcal{O}\left(\lambda_0 L/A\right)$, while the spatial support of the exponential that comes from random effects is $\mathcal{O}\left(\ell_x\lambda_0/\sqrt{\ell_z L}\right)$, thus, the random medium actually improves the resolution if $A \ll L(\sqrt{\ell_z L}/\ell_x)$.

To obtain an explicit expression for the effective aperture we assume that the spatial window has a Gaussian shape $\chi_{\mathrm{x}}(\boldsymbol{x}) = \exp(-|\boldsymbol{x}|^2/2)$, so that

$$\mathbb{E}\big[\breve{\mathcal{K}}(\omega, \boldsymbol{x}, \boldsymbol{x}')\big] = \frac{\chi_{\mathrm{t}}(0)A^2\omega_0^2}{(2\pi c_0 L)^2} e^{i\frac{\omega_0}{c_0}\frac{|\boldsymbol{x}|^2-|\boldsymbol{x}'|^2}{2L}} e^{\frac{\omega_0^2}{c_0^2}\left(\frac{L\ell_z\tilde{C}_0''(0)}{24\ell_x^2}-\frac{A^2}{2L^2}\right)|\boldsymbol{x}-\boldsymbol{x}'|^2},$$

and we also assume that the original source has a Gaussian shape with radius r_0: $\boldsymbol{J}(s, \boldsymbol{x}) = \boldsymbol{J}(s)\exp[-|\boldsymbol{x}|^2/(2r_0^2)]$. We then find that the mean refocused field is

$$\mathbb{E}\big[E_j^{(\mathrm{ref})}(s, \boldsymbol{x})\big] = \frac{\chi_{\mathrm{t}}(0)A^2\omega_0^2\zeta_0 J_{\mathrm{eff},j}(s)}{4c_0^2L^2(r_0^{-2}+r_1^{-2}+ir_2^{-2})} e^{-\frac{|\boldsymbol{x}|^2}{2r_1^2}\frac{r_0^{-2}(r_0^{-2}+r_1^{-2})+r_2^{-4}}{(r_0^{-2}+r_1^{-2})^2+r_2^{-2}}} e^{i\frac{|\boldsymbol{x}|^2}{2r_2^2}\frac{r_0^{-4}+2r_0^{-2}r_1^{-2}+r_2^{-4}}{(r_0^{-2}+r_1^{-2})^2+r_2^{-2}}},$$

where (for $j = 1, 2$)

$$J_{\mathrm{eff},j}(s) = \left(B_{j1}^{(1)}A_{j1}^{(1)} - B_{j2}^{(2)}A_{j2}^{(2)}\right) J_1(-s) + \left(B_{j2}^{(1)}A_{j2}^{(1)} + B_{j2}^{(2)}A_{j2}^{(2)}\right) J_2(-s), \quad (7.10)$$

and

$$r_1 = \frac{c_0 L}{\omega_0 A_{\mathrm{eff}}}, \quad A_{\mathrm{eff}} = \sqrt{A^2 + \frac{|\tilde{C}_0''(0)|\ell_z L^3}{12\ell_x^2}}, \quad r_2^2 = \frac{c_0 L}{\omega_0}. \quad (7.11)$$

If the initial source is point-like $r_0 \to 0$, then we have simply

$$\mathbb{E}\big[E_j^{(\mathrm{ref})}(s, \boldsymbol{x})\big] \simeq \frac{\chi_{\mathrm{t}}(0)A^2\omega_0^2\zeta_0 r_0^2 J_{\mathrm{eff},j}(s)}{4c_0^2L^2} e^{-\frac{|\boldsymbol{x}|^2}{2r_1^2}} e^{i\frac{|\boldsymbol{x}|^2}{2r_2^2}}. \quad (7.12)$$

This corresponds to a refocusing spot size given by the effective Rayleigh resolution formula $\lambda_0 L/A_{\text{eff}}$ for A_{eff} the effective TRM size enhanced by the random medium as in the scalar case [8, 28].

Note that:

• We have only discussed the refocused mean field. In fact, in a regime of large lateral diversity the realization-dependent fluctuations around the mean signal are small and the refocused profile is self-averaging [29].

• The effective TRM size and the refocusing enhancement due to the random medium is independent of the "scrambling" of the modes at the TRM. It is now clear that one can record only one component of the electromagnetic field and use this signal as a source and still experience superfocusing ! Only a very particular combination of the recorded electromagnetic signal cancels the effective source $\boldsymbol{J}_{\text{eff}}$ in (7.10), and all other combinations generate a refocused field with the same spatial profile. Our paraxial representation that articulates the correlation between modes gives directly this result and therefore that time reversal in our configuration can be carried out in a robust fashion. The central and novel aspect of our representation is that we have obtained a joint representation for the modes that involves one, common, Brownian motion which reflects the fact that the modes are associated with the same speed of propagation and "sense" the medium fluctuations in the same way.

7.3. Coherence, wave spectrum, and imaging. An emerging portfolio of techniques involves imaging in heterogeneous media by exploiting coherence phenomena in wave fields that is due to fine scale heterogeneities in order to image macro scale features. We believe that our results are important to develop such techniques in the context of electromagnetic waves.

In Section 7.1 we discussed the interesting physical phenomenon of enhanced backscattering. This phenomenon can have a practical application in the context of tomography in scattering media [34]. Indeed, it follows from our description that the observation of the width of the diffusive cone and of the enhanced backscattering cone can be used for estimation of the scattering coefficient D_0 and the interface location L. The use of the observed cone for imaging purposes is explored numerically in the context of elecromagnetic waves in [13]. Our analysis in Section 7.1 describes the coupling between the medium parameters and the cone parameters which facilitates the use of the cone for imaging purposes. In [13] it was in particular explored numerically how the use of polarization may affect the stability of the cone enhancement. Our analysis was performed in the context of the far field. The technique is relevant also in the near field where the cone dynamics becomes important [2, 3].

The Itô-Schrödinger model can also be used to analyze the cross correlations of signals emitted by ambient noise sources and recorded by a sensor array. The computation of cross correlations can be interpreted as a passive time reversal experiment since both situations involve a product of propagation operators (or Green's functions) with one of them being complex-conjugated. Therefore, in both situations the Wigner distribution of the field plays a critical role. Cross correlations of noisy signals can be used for travel time estimation and applied for tomographic imaging [11, 23].

8. Conclusion. In this paper we have used invariant imbedding and diffusion approximation theorems to study the white-noise parabolic approximation for electromagnetic wave propagation. We have shown that in a scaling regime the transmitted and reflected wave fields are determined by a system of Schrödinger equations driven by a Brownian field. It is the *same* Brownian field in the Schrödinger equations that gives the weak description of the transmission and reflection operators. Thus, only

one Brownian field is needed to describe the joint statistics of the electric and magnetic components of the wave field. The covariance function of this single driving Brownian field is determined in terms of the two-point statistics of the fluctuations of the dielectric permittivity and the magnetic permeability. In particular the enhanced backscattering phenomenon can be analyzed in this regime and we provide explicit formulas for the width of the diffusive specular cone and the one of the enhanced backscattering cone. The enhanced backscattering phenomenon and more generally wave spectral information of the reflected wave can be used for imaging purposes and for the analysis of such problems our representation is important. The limit description that we obtain for the transmission and reflection operators also allows us to analyze time reversal of electromagnetic waves in a random medium and the associated refocusing resolution. The fact that only one Brownian field is involved means that this process is robust with respect to the number and type of components of the electromagnetic field that are recorded.

Many interesting open questions remain and we believe that our paper represents a important step in the direction of development, from first principles, of a framework for description of electromagnetic waves in media with scale separation. Important generalizations involve in particular the case of smoothly varying macroscale medium parameters and scattering of complex geometries.

Acknowledgments. This work was supported in part by the ANR project MIRTEC, DARPA grant N00014-05-1-0442, and NSF grant DMS0709389.

Appendix A. Expressions of the matrices. The matrices $\mathbf{B}^j$ are defined by

$$\mathbf{B}^0 = \frac{i\omega}{2c_0}\begin{bmatrix}1&0&0&0\\0&-1&0&0\\0&0&1&0\\0&0&0&-1\end{bmatrix}, \quad \mathbf{B}^{-2} = \frac{i\omega}{2c_0}\begin{bmatrix}0&1&0&0\\0&0&0&0\\0&0&0&1\\0&0&0&0\end{bmatrix}, \qquad \mathbf{B}^2 = -\big(\mathbf{B}^{-2}\big)^T.$$

The matrices $\breve{\mathbf{A}}^j$ are obtained from $\widehat{\mathbf{A}}^j$ by substitutions $i\kappa_x \to \frac{\partial}{\partial x}$ and $i\kappa_y \to \frac{\partial}{\partial y}$ and we have:

$$\widehat{\mathbf{A}}^0 = \frac{ic_0(\kappa_x^2+\kappa_y^2)}{2\omega}\begin{bmatrix}-1&0&0&0\\0&1&0&0\\0&0&-1&0\\0&0&0&1\end{bmatrix},$$

$$\widehat{\mathbf{A}}^{-2} = \frac{ic_0}{2\omega}\begin{bmatrix}0&\kappa_x^2-\kappa_y^2&0&2\kappa_x\kappa_y\\0&0&0&0\\0&2\kappa_x\kappa_y&0&\kappa_y^2-\kappa_x^2\\0&0&0&0\end{bmatrix}, \quad \widehat{\mathbf{A}}^2 = -(\widehat{\mathbf{A}}^{-2})^T.$$

Appendix B. An invariant imbedding theorem. Let us consider the two-point boundary value problem for $\boldsymbol{X}(z) \in \mathbb{R}^m$:

$$\frac{\mathrm{d}\boldsymbol{X}}{\mathrm{d}z}(z) = \mathbf{A}(z)\boldsymbol{X}(z), \qquad 0 \le z \le L, \tag{B.1}$$

with the boundary condition

$$\mathbf{K}^0\boldsymbol{X}(0) + \mathbf{K}^L\boldsymbol{X}(L) = \boldsymbol{V}^0. \tag{B.2}$$

Here $\mathbf{A}(z)$, $\mathbf{K}^0$, and $\mathbf{K}^L$ are $m \times m$-matrices and $\boldsymbol{V}^0$ is an m-dimensional vector. In this linear framework the invariant imbedding approach leads to the following proposition [6].

PROPOSITION B.1. *Let us assume that $\mathbf{K}^0 + \mathbf{K}^L$ is invertible. Let us define the matrices $(\mathbf{R}(\zeta))_{0\leq\zeta\leq L}$ and $(\mathbf{Q}(z,\zeta))_{0\leq z\leq\zeta\leq L}$ as the solutions of the initial value-problems:*

$$\frac{\mathrm{d}\mathbf{R}}{\mathrm{d}\zeta}(\zeta) = \mathbf{A}(\zeta)\mathbf{R}(\zeta) - \mathbf{R}(\zeta)\mathbf{K}^L\mathbf{A}(\zeta)\mathbf{R}(\zeta), \qquad 0 \leq \zeta \leq L, \tag{B.3}$$

starting from $\zeta = 0$: $\mathbf{R}(\zeta = 0) = (\mathbf{K}^0 + \mathbf{K}^L)^{-1}$, and

$$\frac{\partial\mathbf{Q}}{\partial\zeta}(z,\zeta) = -\mathbf{Q}(z,\zeta)\mathbf{K}^L\mathbf{A}(\zeta)\mathbf{R}(\zeta), \qquad 0 \leq z \leq \zeta \leq L, \tag{B.4}$$

starting from $\zeta = z$: $\mathbf{Q}(z,\zeta = z) = \mathbf{R}(z)$. Then $\mathbf{P}(z) = \mathbf{Q}(z,L)$ is the solution of:

$$\frac{\mathrm{d}\mathbf{P}}{\mathrm{d}z}(z) = \mathbf{A}(z)\mathbf{P}(z), \qquad 0 \leq z \leq L,$$

with the two-point boundary conditions

$$\mathbf{K}^0\mathbf{P}(0) + \mathbf{K}^L\mathbf{P}(L) = \mathbf{I},$$

and consequently $\boldsymbol{X}(z) = \mathbf{P}(z)\boldsymbol{V}^0$ is the solution of (B.1) with the boundary condition (B.2).

REFERENCES

[1] M. Asch, W. Kohler, G. Papanicolaou, M. Postel, and B. White, Frequency content of randomly scattered signals, SIAM Rev., **33**, (1991), pp. 519-625.

[2] A. Aubry, A. Derode, A. Derode, and F. Padilla, Local measurements of the diffusion constant in multiple scattering media: Application to human trabecular bone imaging, Appl. Phys. Lett., **92**, (2008), 124101.

[3] A. Aubry and A. Derode, Ultrasonic imaging of highly scattering media from local measurements of the diffusion constant: Separation of coherent and incoherent intensities, Phys. Rev. E, **75**, (2007), 026602.

[4] F. Bailly, J.-F. Clouet, and J.-P. Fouque, Parabolic and white noise approximation for waves in random media, SIAM J. Appl. Math., **56** (1996), pp. 1445-1470.

[5] Y.N. Barabanenkov, Wave corrections for the transfer equation for backward scattering, Izv. Vyssh. Uchebn. Zaved. Radiofiz., **16**, (1973), pp. 88-96.

[6] R. Bellman and G.M. Wing, Introduction to invariant imbedding, Wiley, New York, 1975.

[7] M.J. Beran and J. Oz-Vogt, Imaging through turbulence in the atmosphere, Prog. Optics, **33**, (1994), pp. 319-388.

[8] P. Blomgren, G. Papanicolaou, and H. Zhao, Super-resolution in time-reversal acoustics, J. Acoust. Soc. Am., **111**, (2002), pp. 230-248.

[9] J. F. Claerbout, Coarse grid calculations of waves in inhomogeneous media with application to delineation of complicated seismic structure, Geophysics, **35**, (1970), pp. 407-418.

[10] D. Dawson and G. Papanicolaou, A random wave process, Appl. Math. Optim., **12**, (1984), pp. 97-114.

[11] M. de Hoop and K. Sølna, Estimating a Green's function from field-field correlations in a random medium, SIAM J. Appl. Math., in print, (2008).

[12] J. de Rosny, A. Tourin, and M. Fink, Coherent backscattering of an elastic wave in a chaotic cavity, Phys. Rev. Lett., **84**, (2000), pp. 1693-1695.

[13] H. El-Ocla, Backscattering enhancement analysis for targets in continuous random media based on wave polarization, Waves in Random and Complex and Media, **18**, (2008), pp. 13-25.

[14] A. Fannjiang, Self-averaging scaling limits for random parabolic waves, Arch. Rational Mech. Anal., **175**, (2005), pp. 343-387.

[15] A. C. Fannjiang and K. Sølna, Superresolution and duality for time-reversal of waves in random media, Phys. Lett. A, **352**, (2005), pp. 22-29.
[16] A. Fannjiang and K. Sølna, Propagation and time-reversal of wave beams in atmospheric turbulence, SIAM Multiscale Model. Simul., **3**, (2005), pp. 522-558.
[17] M. Fink, Time reversed acoustics, Physics Today, **20**, (1997), pp. 34-40.
[18] V.A. Fock, Electromagnetic diffraction and propagation problems, Pergamon, New York ,1965.
[19] J.-P. Fouque, J. Garnier, G. Papanicolaou, and K. Sølna, Wave propagation and time reversal in randomly layered media, Springer, New York, 2007.
[20] J.-P. Fouque, G. Papanicolaou, and Y. Samuelides, Forward and Markov approximation: the strong-intensity-fluctuations regime revisited, Waves in Random Media, **8**, (1998), pp. 303-314.
[21] K. Furutsu, Random media and boundaries: unified theory, two-scale method, and applications, Springer-Verlag, Berlin, 1993.
[22] C.W. Gardiner, Handbook of stochastic methods, Springer, Berlin, 2004.
[23] J. Garnier and G. Papanicolaou, Passive sensor imaging using cross correlations of noisy signals in a scattering medium, to appear in SIAM J. Imaging Sciences, available at http://www.proba.jussieu.fr/˜garnier/
[24] J. Garnier and K. Sølna, Coupled paraxial wave equations in random media in the white-noise regime, to appear in Ann. Appl. Probab., available via http://www.proba.jussieu.fr/˜garnier/
[25] W. Kohler, G. Papanicolaou, M. Postel, and B. White, Reflection of pulsed electromagnetic waves from a randomly stratified half-space, J. Opt. Soc. Am. A, **8**, (1991), pp. 1109-1125.
[26] M. Levy, Parabolic equation methods for electromagnetic wave propagation, The Institution of Electrical Engineers, London, 2000.
[27] A.A. Maradudin, J.Q. Lu, T. Michel, Z. Gu, J.C. Dainrt, A.J. Sant, E.R. Mendez and M. Nieto-Vesperinas, Enhanced backscattering and transmission of light from random surfaces on semi-infinite substrates and thin films, Waves in random Media, **3**, (1991), pp. S129-S141.
[28] G. Papanicolaou, L. Ryzhik, and K. Sølna, Statistical stability in time reversal, SIAM J. Appl. Math., **64**, (2004), pp. 1133-1155.
[29] G. Papanicolaou, L. Ryzhik, and K. Sølna, Self-averaging from lateral diversity in the Itô-Schrödinger equation, SIAM Multiscale Model. Simul., **6**, (2007), pp. 468-492.
[30] M.C.W. van Rossum and Th.M. Nieuwenhuizen, Multiple scattering of classical waves: microscopy, mesoscopy, and diffusion, Rev. Mod. Phys., **71**, (1999), pp. 313-371.
[31] J.W. Strohbehn (ed.), Laser beam propagation in the atmosphere, Springer, Berlin, 1978.
[32] F. Tappert, The parabolic approximation method, in Wave propagation and underwater acoustics, J.B. Keller and J.S. Papadakis (eds.), pp. 224-287, Springer, Berlin, 1977.
[33] V.I. Tatarski, The effects of the turbulent atmosphere on wave propagation, U.S. Department of Commerce, Springfield, VA, 1971.
[34] L. Thrane, H.T. Yura, and P.E. Andersen, Analysis of optical coherence tomography systems based on the extended Huygens-Fresnel principle, J. Opt. Soc. Am. A, **17**, (2000), pp. 484-490.
[35] R.L. Weaver and O.I. Lobkis, Enhanced backscattering and modal echo of reverberant elastic waves, Phys. Rev. Lett., **84**, (2000), pp. 4942-4945.